Partition-Insensitive Parallel ADMM Algorithm for High-dimensional Linear Models

Xiaofei Wu
College of Mathematics and Statistics, Chongqing University, and
Zhimin Zhang *
College of Mathematics and Statistics, Chongqing University.

September 18, 2023

Abstract

The parallel alternating direction method of multipliers (ADMM) algorithms have gained popularity in statistics and machine learning for their efficient handling of large sample data problems. However, the parallel structure of these algorithms is based on the consensus problem, which can lead to an excessive number of auxiliary variables for high-dimensional data. In this paper, we propose a partition-insensitive parallel framework based on the linearized ADMM (LADMM) algorithm and apply it to solve nonconvex penalized smooth quantile regression problems. Compared to existing parallel ADMM algorithms, our algorithm does not rely on the consensus problem, resulting in a significant reduction in the number of variables that need to be updated at each iteration. It is worth noting that the solution of our algorithm remains unchanged regardless of how the total sample is divided, which is also known as partition-insensitivity. Furthermore, under some mild assumptions, we prove that the iterative sequence generated by the parallel LADMM algorithm converges to a critical point of the nonconvex optimization problem. Numerical experiments on synthetic and real datasets demonstrate the feasibility and validity of the proposed algorithm.

Keywords: Global convergence; Nonconvex optimization; Parallel algorithm; Robust regression; LADMM

^{*}Corresponding author. Email: zmzhang@cqu.edu.cn. The research of Zhimin Zhang was supported by the National Natural Science Foundation of China [Grant Numbers 12271066, 12171405, 11871121], and the research of Xiaofei Wu was supported by the Scientific and Technological Research Program of Chongqing Municipal Education Commission [Grant Numbers KJQN202302003].

1 Introduction

High-dimensional linear regression model can be written as the form of " loss + penalty",

$$\underset{\boldsymbol{\beta} \in \mathbb{R}^p}{\operatorname{arg\,min}} \quad \frac{1}{n} \sum_{i=1}^n \mathcal{L}(y_i - \boldsymbol{x}_i^{\top} \boldsymbol{\beta}) + P_{\lambda}(|\boldsymbol{\beta}|), \tag{1}$$

where y_i denotes the *i*-th sample response vector, and $\boldsymbol{x}_i \in \mathbb{R}^p$ denotes the *i*-th sample observation value of covariates. Here, the loss function \mathcal{L} is a generic function that includes least squares, asymmetric least squares (Newey and Powell (1987)), Huber loss (Huber (1964)), quantile loss (Koenker and Basset (1970)), smooth quantile loss (Jennings et al. (1993) and Aravkin et al. (2014)), among others. In this paper, our main focus is on nonconvex penalty terms denoted as $P_{\lambda}(|\boldsymbol{\beta}|)$. These nonconvex penalties include SCAD (Fan and Li (2001)), MCP (Zhang (2010)), capped- ℓ_1 (Zhang (2010)), Snet (Wang et al. (2010)) and Mnet (Huang et al. (2015)).

In the past decade, many parallel ADMM algorithms have been proposed to solve (1) when the sample n is particularly large or the data is stored in a distributed manner, such as Yu and Lin (2017a), Yu et al. (2017b) and Fan et al. (2020). The parallel algorithm is based on the concept of decomposing a complex optimization problem into smaller and more manageable subproblems, which can be solved in parallel on local machines. Assuming that there are a total of M local machines available, the data y and X can be divided into M blocks as follows,

$$\boldsymbol{y} = (\boldsymbol{y}_1^{\mathsf{T}}, \boldsymbol{y}_2^{\mathsf{T}}, \dots, \boldsymbol{y}_M^{\mathsf{T}})^{\mathsf{T}}, \ \boldsymbol{X} = (\boldsymbol{X}_1^{\mathsf{T}}, \boldsymbol{X}_2^{\mathsf{T}}, \dots, \boldsymbol{X}_M^{\mathsf{T}})^{\mathsf{T}},$$
 (2)

where $\mathbf{y}_m \in \mathbb{R}^{n_m}$, $\mathbf{X}_m \in \mathbb{R}^{n_m \times p}$ and $\sum_{m=1}^{M} n_m = n$. To adapt to this parallel structure, the existing parallel ADMM algorithms employ strategies similar to the regularized consensus problem described by Boyd et al. (2010). By introducing the consensus constraints $\{\boldsymbol{\beta} = \boldsymbol{\beta}_m\}_{m=1}^{M}$, the constrained optimization problem of (1) is as follows

$$\min_{\boldsymbol{\beta}, \boldsymbol{r}_{m}, \boldsymbol{\beta}_{m}} \frac{1}{n} \sum_{m=1}^{M} \mathcal{L}(\boldsymbol{r}_{m}) + P_{\lambda}(|\boldsymbol{\beta}|),$$
s.t. $\boldsymbol{X}_{m} \boldsymbol{\beta}_{m} + \boldsymbol{r}_{m} = \boldsymbol{y}_{m}, \ \boldsymbol{\beta} = \boldsymbol{\beta}_{m}, \ m = 1, 2, \dots, M,$ (3)

where $\boldsymbol{r} = (\boldsymbol{r}_1^\top, \boldsymbol{r}_2^\top, \dots, \boldsymbol{r}_M^\top)^\top$ and $\mathcal{L}(\boldsymbol{r}_m) = \sum_i \mathcal{L}(\boldsymbol{r}_{mi})$. To solve the constrained optimization problem (3), both the central and local machines must handle a subproblem with the same dimension as $\boldsymbol{\beta}$ in each iteration. However, in the case of penalized regression, it is common for $\boldsymbol{\beta}$ to have a relatively large dimension. As $\boldsymbol{r} = (\boldsymbol{r}_1^\top, \boldsymbol{r}_2^\top, \dots, \boldsymbol{r}_m^\top)^\top$ and each local machine needs to solve its corresponding $\boldsymbol{\beta}_m$, thus solving parallel problems results in solving at least Mp subproblems more than the nonparallel case.

Although this phenomenon can be mitigated through parallel computing structures, that is, the time required for M local machines to compute Mp subproblems is equivalent to one machine computing p subproblems. Nonetheless, these additional auxiliary variables have a negative impact on the convergence speed and accuracy of the algorithm. This drawback was also emphasized by Lin et al. (2022), and they suggested avoiding excessive auxiliary variables when designing ADMM algorithm. More importantly, $\{\beta_m\}_{m=1}^M$ is not the desired estimation value that we initially aim for, but rather the auxiliary variables added to avoid the need for double loops and facilitate parallel structure, see Yu et al. (2017b) for more details. So a natural question arises: is it possible to design an ADMM algorithm without adding these auxiliary variables, while still maintaining parallel structure and avoiding double loops?

This paper provides a positive answer to this question by designing a parallel algorithm based on LADMM. To enhance the applicability of our proposed algorithm, we choose a very general loss called smooth quantile loss as \mathcal{L} , and incorporate generalized nonconvex penalty terms, namely Snet and Mnet, as the penalty terms $P_{\lambda}(|\beta|)$. Compared to existing related algorithms, our algorithm offers three main advantages:

- Not an approximation algorithm: Our algorithm directly tackles nonnonvex optimization problems without relying on methods like local linear approximation in Zou and Li (2008), majorization minimization step in Yu et al. (2017b), or iterative reweighting in Pan et al. (2021). For smooth quantile losses, our algorithm also directly derives its proximal operator, rather than using first-order approximation methods as in Mkhadri et al. (2017). Additionally, we provide strict theoretical guarantees of global convergence, ensuring that our algorithm converges to a critical point of the nonconvex optimization problem.
- Fewer iterative variables: Compared to existing parallel ADMM algorithms, our parallel

LADMM algorithm requires fewer iterative variables. Existing algorithms typically handle subproblems with dimensions of at least (2M+1)p+2nM, while our algorithm only requires p+2n dimensions. This reduction in the number of variables is especially advantageous when p is large.

• Partition-Insensitive: As stated by Fan et al. (2020), the more local machines there are, the parallel algorithms proposed by Yu et al. (2017b) and Fan et al. (2020) tend to choose more non-zero variables. By contrast, our algorithm ensures that the solution remains the same across different configurations of local machines and the number of samples they process. This consistency ensures the reliability and accuracy of the solutions, regardless of the chosen parallelization strategy.

The remainder of this paper is structured as follows. Section 2 introduces two smooth quantile loss functions and some nonconvex penalties, and derives the closed-form solutions of their proximal operators. In Section 3, we propose the LADMM algorithm for computing nonconvex penalized regression and derive its parallel version. We also explained the equivalence relationship between parallel and nonparallel algorithms and provide the convergence of the algorithms in this section. In Section 4, we present the performance of the proposed algorithm on some synthetic datasets, and compare it with existing methods. Section 5 utilizes the parallel LADMM algorithm to conduct regressions on an online publicly available dataset, leading to the discovery of several new findings. Section 6 summarizes the findings and concludes the paper with a discussion of future research directions. The technical proofs and supplementary numerical experiments are included in the Appendix. R package PIPADMM for implementing the parallel LADMM is available at https://github.com/xfwu1016/PIPADMM.

2 Preliminary

In this section, we introduce the smooth quantile functions and some nonconvex penalties. Combining these two together produces a generalized nonconvex penalized regression model. For the convenience of describing the algorithm, we also derive the closed-form solutions of the proximal operators of smooth quantile functions and nonconvex penalties.

2.1 Smooth Quantile Loss

The quantile loss function, proposed by Koenker and Basset (1970), is defined as

$$\rho_{\tau}(u) = u(\tau - 1_{u < 0})$$

where $\tau \in (0,1)$ and $1_{u<0}$ is an indicator function, which is equal to 1 if u<0, and 0 otherwise. This loss function has been widely studied in linear regression because it can go beyond the typical Gaussian assumptions and effectively resolve heavy-tailed random error distributions. However, the traditional quantile loss function may not be suitable for scenarios with noise and outliers, as it aims for precise fitting of a specific section of the data. Studies conducted by Aravkin et al. (2014) and Mkhadri et al. (2017) have shown the limitations of the traditional quantile loss function and suggest using the smooth quantile loss as a better alternative.

The two popular smooth quantile losses proposed by Jennings et al. (1993) and Aravkin et al. (2014) are respectively defined as follows

$$\mathcal{L}_{\tau,c}(u) = \begin{cases}
\tau(u - 0.5c) & \text{if } u \ge c, \\
\frac{\tau u^2}{2c} & \text{if } u \in [0, c), \\
\frac{(1-\tau)u^2}{2c} & \text{if } u \in [-c, 0), \\
(\tau - 1)(u + 0.5c) & \text{if } u < -c,
\end{cases} \tag{4}$$

and

$$\mathcal{L}_{\tau,\kappa}(u) = \begin{cases}
\tau(u - \frac{\tau\kappa}{2}) & \text{if } u > \tau\kappa, \\
\frac{u^2}{2\kappa} & \text{if } u \in [(\tau - 1)\kappa, \tau\kappa], \\
(\tau - 1)[u - \frac{(\tau - 1)\kappa}{2}] & \text{if } u < (\tau - 1)\kappa,
\end{cases} \tag{5}$$

where $\tau \in (0,1)$, c > 0 and $\kappa > 0$ are three given constants. The smooth quantile loss is called a generalized loss because $\mathcal{L}_{\tau,\kappa}(u)$ and / or $\mathcal{L}_{\tau,\kappa}(u)$ can be almost identical to the quantile loss, least squares loss, asymmetric least squares loss and Huber loss by changing τ , c and κ . Obviously, these two smooth quantile losses are the modified versions of the quantile loss function that incorporates

smooth functions to replace the non-differentiable portion near the origin. This modification allows for differentiability at the origin, making it easier to analyze theoretically and design algorithms. One manifestation is that $\mathcal{L}_{\tau,*}(u)$ has Lipschitz continuous first derivatives, while quantile loss does not.

Because of these advantages and flexibility, smooth quantile loss is widely used in various fields, such as nonparametric regression (Hee-Seok et al. (2011)), functional data clustering (Kim and Oh (2020)), linear regression (Zheng (2011)), and penalized linear regression (Ouhourane et al. (2022)). Several algorithms have been proposed to handle smooth quantile regression (with or without penalty terms), including gradient descent algorithms (Zheng (2011)), orthogonal matching pursuit (Aravkin et al. (2014)), and coordinate descent (Mkhadri et al. (2017)). It is important to note that the aforementioned algorithms primarily concentrate on convex penalties. Although Mkhadri et al. (2017) extended the algorithm to nonconvex cases, its theoretical convergence is not guaranteed. To the best of our knowledge, no ADMM algorithm has been introduced specifically for solving regression models with smooth quantile regression.

2.2 Nonconvex Penalized Smooth Quantile Regression

Next, we introduce two generalized nonconvex penalties, namely Snet (Wang et al. (2010)) and Mnet (Huang et al. (2015)), and additionally propose a novel nonconvex penalty, called Cnet. Mnet is a combination of MCP and ridge, and Snet is a combination of SCAD and ridge, that is,

$$Snet(\boldsymbol{\beta}) = MCP_{\lambda_1}(\boldsymbol{\beta}) + \frac{\lambda_2}{2} \|\boldsymbol{\beta}\|_2^2,$$
$$Mnet(\boldsymbol{\beta}) = SCAD_{\lambda_1}(\boldsymbol{\beta}) + \frac{\lambda_2}{2} \|\boldsymbol{\beta}\|_2^2.$$

The capped- ℓ_1 is proposed by Zhang (2010) and has received some attention in Guan et al. (2018) and Pan et al. (2021), which is defined as $\lambda_1 \sum_j \min\{|\beta_j|, a\}$. Then, the Cnet is defined as

$$\operatorname{Cnet}(\boldsymbol{\beta}) = \lambda_1 \sum_{j} \min\{|\beta_j|, a\} + \frac{\lambda_2}{2} \|\boldsymbol{\beta}\|_2^2, \tag{6}$$

where a is a given constant.

Combining the smooth quantile loss and the generalized nonconvex penalty together produces

a generalized nonconvex penalized regression model,

$$\underset{\boldsymbol{\beta} \in \mathbb{R}^p}{\operatorname{arg\,min}} \quad \frac{1}{n} \sum_{i=1}^n \mathcal{L}_{\tau,*}(y_i - \boldsymbol{x}_i^{\top} \boldsymbol{\beta}) + P_{\lambda}(|\boldsymbol{\beta}|). \tag{7}$$

We abbreviate it as NPSQR. NPSQR is a special case of regularized M-estimator, and its statistical properties have been studied in many scenarios, as shown in Negahban et al. (2010), Li et al. (2011), Loh and Wainwright (2015), Loh (2017) and Zhou et al. (2018).

2.3 Proximal Operator

To facilitate the closed-form solutions for the updates of β and r in the ADMM algorithm, we will introduce the following proximal operators,

$$\operatorname{prox}_{\mu,g}(\boldsymbol{v}) = \arg\min_{\boldsymbol{u}} \left\{ g(\boldsymbol{u}) + \frac{\mu}{2} \|\boldsymbol{u} - \boldsymbol{v}\|_{2}^{2} \right\}, \tag{8}$$

where $g(\boldsymbol{u})$ is a nonnegative real-valued mapping function, \boldsymbol{v} is a constant vector, and $\mu > 0$ is a constant. In this paper, the function $g(\boldsymbol{u})$ is separable, that is, $g(\boldsymbol{u}) = \sum_j g(u_j)$. Then, we can divide the optimization problem (8) in to multiple independent univariate problems. Here, we introduce the proximal operators of the aforementioned losses and penalties, which play a crucial role in our algorithm. The detailed derivation process of these closed-form solutions is provided in Appendix A. We are not aware of any prior work that has derived closed-form solutions for these operators (except for Snet in Wang et al. (2010)), making our contribution novel in this regard. Furthermore, our derivation method is concise and easily extendable, enabling potential applications beyond the scope of this study.

• The proximal operator of $\mathcal{L}_{\tau,c}(\boldsymbol{u})$

$$\operatorname{prox}_{\mu,\mathcal{L}_{\tau,c}}(\boldsymbol{v}_{j}) = \begin{cases} \boldsymbol{v}_{j} - \frac{\tau}{n\mu}, & \text{if } \boldsymbol{v}_{j} \geq c + \frac{\tau}{n\mu}, \\ \frac{nc\mu\boldsymbol{v}_{j}}{nc\mu+\tau}, & \text{if } 0 \leq \boldsymbol{v}_{j} < c + \frac{\tau}{n\mu}, \\ \frac{nc\mu\boldsymbol{v}_{j}}{nc\mu+1-\tau}, & \text{if } -c + \frac{\tau-1}{n\mu} \leq \boldsymbol{v}_{j} < 0, \\ \boldsymbol{v}_{j} - \frac{\tau-1}{n\mu}, & \text{if } \boldsymbol{v}_{j} < -c + \frac{\tau-1}{n\mu}. \end{cases}$$
(9)

• The proximal operator of $\mathcal{L}_{\tau,\kappa}(u)$

$$\operatorname{prox}_{\mu,\mathcal{L}_{\tau,\kappa}}(\boldsymbol{v}_{j}) = \begin{cases} \boldsymbol{v}_{j} - \frac{\tau}{n\mu}, & \text{if } \boldsymbol{v}_{j} \geq \tau\kappa + \frac{\tau}{n\mu}, \\ \frac{n\kappa\mu\boldsymbol{v}_{j}}{n\kappa\mu + 1}, & \text{if } (\tau - 1)\kappa + \frac{\tau - 1}{n\mu} \leq \boldsymbol{v}_{j} < \tau\kappa + \frac{\tau}{n\mu}, \\ \boldsymbol{v}_{j} - \frac{\tau - 1}{n\mu}, & \text{if } \boldsymbol{v}_{j} < (\tau - 1)\kappa + \frac{\tau - 1}{n\mu}. \end{cases}$$
(10)

Obviously, when c = 0 and $\kappa = 0$, the proximal operators of quantile loss in Gu et al. (2017) is a special case in (9) or (10).

• The proximal operator of Snet with $(a-1)(\eta + \lambda_2) > 1$:

$$\operatorname{prox}_{\eta, P_{\lambda}}(\boldsymbol{v}_{j}) = \begin{cases} \operatorname{sign}(\boldsymbol{v}_{j}) \cdot \left[\frac{\eta |\boldsymbol{v}_{j}| - \lambda_{1}}{\eta + \lambda_{2}}\right]_{+}, & \text{if } |\boldsymbol{v}_{j}| \leq \frac{\lambda_{1}(1 + \eta + \lambda_{2})}{\eta}, \\ \operatorname{sign}(\boldsymbol{v}_{j}) \cdot \left[\frac{(a - 1)\eta |\boldsymbol{v}_{j}| - a\lambda_{1}}{(a - 1)(\eta + \lambda_{2}) - 1}\right]_{+}, & \text{if } \frac{\lambda_{1}(1 + \eta + \lambda_{2})}{\eta} < |\boldsymbol{v}_{j}| < \frac{a\lambda_{1}(\eta + \lambda_{2})}{\eta}, \\ \frac{\eta \boldsymbol{v}_{j}}{\eta + \lambda_{2}}, & \text{if } |\boldsymbol{v}_{j}| \geq \frac{a\lambda_{1}(\eta + \lambda_{2})}{\eta}. \end{cases}$$
(11)

Note that $(a-1)(\eta + \lambda_2) > 1$ is always valid in this paper, as a = 3.7 and $\eta >> 1$. When $\eta = 1$, the solution in (11) is the same as the solution mentioned in Wang et al. (2010).

• The proximal operator of Mnet:

$$\operatorname{prox}_{\eta, P_{\lambda}}(\boldsymbol{v}_{j}) = \begin{cases} \operatorname{sign}(\boldsymbol{v}_{j}) \cdot \left[\frac{a\eta|\boldsymbol{v}_{j}| - a\lambda_{1}}{a(\eta + \lambda_{2}) - 1}\right]_{+}, & \text{if } |\boldsymbol{v}_{j}| < \frac{a\lambda_{1}(\eta + \lambda_{2})}{\eta}, \\ \frac{\eta\boldsymbol{v}_{j}}{\eta + \lambda_{2}}, & \text{if } |\boldsymbol{v}_{j}| \geq \frac{a\lambda_{1}(\eta + \lambda_{2})}{\eta}. \end{cases}$$
(12)

Obviously, when $\lambda_2 = 0$, the proximal operators of SCAD in Fan and Li (2001) and MCP in Zhang (2010) are special cases in (12) and (11), respectively.

• The proximal operator of Cnet:

$$\operatorname{prox}_{\eta, P_{\lambda}}(\boldsymbol{v}_{j}) = \begin{cases} \operatorname{sign}(\boldsymbol{v}_{j}) \cdot \left[\frac{\eta |\boldsymbol{v}_{j}| - \lambda_{1}}{\eta + \lambda_{2}}\right]_{+}, & \text{if } |\boldsymbol{v}_{j}| < \frac{a(\eta + \lambda_{2})}{\eta}, \\ \frac{\eta \boldsymbol{v}_{j}}{\eta + \lambda_{2}}, & \text{if } |\boldsymbol{v}_{j}| \geq \frac{a(\eta + \lambda_{2})}{\eta}. \end{cases}$$
(13)

3 The Parallel LADMM Algorithm

In general, ADMM is an algorithm to solve a problem that features a two-bolck separable objective functions but connects equality constraints. Setting $\mathbf{r} = \mathbf{y} - \mathbf{X}\boldsymbol{\beta}$, the NPSQR problems in (7) can be transformed into

$$\min_{\boldsymbol{\beta}, \boldsymbol{r}} \quad \sum_{i=1}^{n} \mathcal{L}_{\tau, *}(r_i) + P_{\lambda}(|\boldsymbol{\beta}|),$$
s.t. $\boldsymbol{X}\boldsymbol{\beta} + \boldsymbol{r} = \boldsymbol{y}$. (14)

Problem (14) has the following augmented Lagrangian,

$$L_{\mu}(\boldsymbol{\beta}, \boldsymbol{r}, \boldsymbol{d}) = \mathcal{L}_{\tau,*}(\boldsymbol{r}) + P_{\lambda}(|\boldsymbol{\beta}|) - \boldsymbol{d}^{\top}(\boldsymbol{X}\boldsymbol{\beta} + \boldsymbol{r} - \boldsymbol{y}) + \frac{\mu}{2} \|\boldsymbol{X}\boldsymbol{\beta} + \boldsymbol{r} - \boldsymbol{y}\|_{2}^{2},$$
(15)

where $d \in \mathbb{R}^n$ is the dual variable, and $\mu > 0$ is a tunable augmentation parameter. The ADMM algorithm alternates between the following iterative steps with given r^0 and d^0 ,

$$\begin{cases}
\boldsymbol{\beta}^{k+1} = \underset{\boldsymbol{\beta}}{\operatorname{arg\,min}} \left\{ P_{\lambda}(|\boldsymbol{\beta}|) + \frac{\mu}{2} \left\| \boldsymbol{X}\boldsymbol{\beta} + \boldsymbol{r}^{k} - \boldsymbol{y} - \boldsymbol{d}^{k}/\mu \right\|_{2}^{2} \right\}, \\
\boldsymbol{r}^{k+1} = \underset{\boldsymbol{r}}{\operatorname{arg\,min}} \left\{ \mathcal{L}_{\tau,*}(\boldsymbol{r}) + \frac{\mu}{2} \left\| \boldsymbol{X}\boldsymbol{\beta}^{k+1} + \boldsymbol{r} - \boldsymbol{y} - \boldsymbol{d}^{k}/\mu \right\|_{2}^{2} \right\}, \\
\boldsymbol{d}^{k+1} = \boldsymbol{d}^{k} - \mu(\boldsymbol{X}\boldsymbol{\beta}^{k+1} + \boldsymbol{r}^{k+1} - \boldsymbol{y}).
\end{cases} (16)$$

Similar iterative schemes have been used by Yu et al. (2017b) and Gu et al. (2017) to solve the convex penalized quantile regression. However, the β -update in (16) is a regression problem similar to penalized least squares, which does not have a closed-form solution. This update is computationally expensive because it requires numerical optimization techniques such as coordinate descent, resulting in a double-loop algorithm. Next, we will introduce the LADMM algorithm to solve this issue.

3.1 LADMM Algorithm

The LADMM algorithms have been widely applied in convex sparse statistical learning models, such as dantzig selector in Wang and Yuan (2012), sparse group and fused Lasso in Li et al. (2014),

sparse quantile regression in Gu et al. (2017). The core concept behind the LADMM algorithm is to linearize the quadratic term and thus generate a proximal operator. This is achieved by implementing the following iteration,

$$\begin{cases}
\boldsymbol{\beta}^{k+1} = \underset{\boldsymbol{\beta}}{\operatorname{arg min}} \left\{ P_{\lambda}(|\boldsymbol{\beta}|) + \frac{\mu}{2} \| \boldsymbol{X}\boldsymbol{\beta} + \boldsymbol{r}^{k} - \boldsymbol{y} - \boldsymbol{d}^{k}/\mu \|_{2}^{2} + \frac{1}{2} \| \boldsymbol{\beta} - \boldsymbol{\beta}^{k} \|_{S}^{2} \right\}, \\
\boldsymbol{r}^{k+1} = \underset{\boldsymbol{r}}{\operatorname{arg min}} \left\{ \mathcal{L}_{\tau,*}(\boldsymbol{r}) + \frac{\mu}{2} \| \boldsymbol{X}\boldsymbol{\beta}^{k+1} + \boldsymbol{r} - \boldsymbol{y} - \boldsymbol{d}^{k}/\mu \|_{2}^{2} \right\}, \\
\boldsymbol{d}^{k+1} = \boldsymbol{d}^{k} - \mu(\boldsymbol{X}\boldsymbol{\beta}^{k+1} + \boldsymbol{r}^{k+1} - \boldsymbol{y}),
\end{cases} (17)$$

where $S = \eta I_p - \mu X^{\top} X$. To ensure the convergence of the algorithm, we need S to be a positive-definite matrix, i.e., $\eta > \text{eigen}(\mu \mathbf{X}^{\top} \mathbf{X})$, where $\text{eigen}(\mu \mathbf{X}^{\top} \mathbf{X})$ is the maximum eigenvalue of $\mu \boldsymbol{X}^{\top} \boldsymbol{X}$.

Algorithm 1 LADMM for solving NPSQR.

Input: Observation data X, y; primal variables β^0, r^0 ; dual variables d^0 ; augmented parameters μ ; penalty parameter λ_1 and λ_2 ; and selectable parameters $\tau \in (0,1)$ and c or $\kappa > 0$.

Output: The last iteration solution β^K .

Calculate: $\eta = eigen(\mu X^{\top} X)$.

while not converged do

1. Update
$$\boldsymbol{\beta}_{j}^{k+1} = \operatorname{prox}_{\eta, P_{\lambda}} \left(\boldsymbol{\beta}_{j}^{k} - \frac{\left[\mu \boldsymbol{X}^{\top} (\boldsymbol{X} \boldsymbol{\beta}^{k} + \boldsymbol{r}^{k} - \boldsymbol{y} - \boldsymbol{d}^{k} / \mu) \right]_{j}}{\eta} \right), j = 1, 2, \dots, p,$$

2. Update
$$\mathbf{r}_{i}^{k+1} = \text{prox}_{\mu, \mathcal{L}_{\tau, *}} ([\mathbf{y} + \mathbf{d}^{k}/\mu - \mathbf{X}\boldsymbol{\beta}^{k+1}]_{i}), i = 1, 2, \dots, n,$$

3. Update $\mathbf{d}^{k+1} = \mathbf{d}^{k} - \mu(\mathbf{X}\boldsymbol{\beta}^{k+1} + \mathbf{r}^{k+1} - \mathbf{y}).$

end while

return solution

For the β -update, we ignore the constant term, and the subproblems becomes

$$\boldsymbol{\beta}^{k+1} = \underset{\boldsymbol{\beta}}{\operatorname{arg\,min}} \left\{ P_{\lambda}(|\boldsymbol{\beta}|) + \frac{\eta}{2} \left\| \boldsymbol{\beta} - \boldsymbol{\beta}^{k} + \frac{\mu \boldsymbol{X}^{\top} (\boldsymbol{X} \boldsymbol{\beta}^{k} + \boldsymbol{r}^{k} - \boldsymbol{y} - \boldsymbol{d}^{k}/\mu)}{\eta} \right\|_{2}^{2} \right\}.$$
(18)

Obviously, both $\boldsymbol{\beta}^{k+1}$ and \boldsymbol{r}^{k+1} can be represented as proximal operators, that is,

$$\begin{cases}
\boldsymbol{\beta}^{k+1} = \operatorname{prox}_{\eta, P_{\lambda}} \left(\boldsymbol{\beta}^{k} - \frac{\mu \boldsymbol{X}^{\top} (\boldsymbol{X} \boldsymbol{\beta}^{k} + \boldsymbol{r}^{k} - \boldsymbol{y} - \boldsymbol{d}^{k} / \mu)}{\eta} \right), \\
\boldsymbol{r}^{k+1} = \operatorname{prox}_{\mu, \mathcal{L}_{\tau, *}} \left(\boldsymbol{y} + \boldsymbol{d}^{k} / \mu - \boldsymbol{X} \boldsymbol{\beta}^{k+1} \right).
\end{cases} (19)$$

To summarize, the iterative scheme of LADMM for (14) can be described in Algorithm 1.

3.2 Parallel LADMM Algorithm

This subsection focuses on the implementation of parallel LADMM algorithms for large-scale data. The main objective is to solve the problem in a distributed manner, with each processor handling a subset of the training data. This distributed approach proves advantageous when dealing with a large number of training examples that cannot be feasibly processed on a single machine, or when the data is naturally distributed or stored in such a manner.

Central machine $Update \ \boldsymbol{\beta}^{k+1}$ \mathcal{E}_{1}^{k+1} \mathcal{E}_{1}^{k+1} \mathcal{E}_{1}^{k+1} \mathcal{E}_{1}^{k+1} \mathcal{E}_{1}^{k+1} \mathcal{E}_{1}^{k+1} \mathcal{E}_{1}^{k+1} \mathcal{E}_{1}^{k+1} \mathcal{E}_{1}^{k+1} \mathcal{E}_{2}^{k+1} \mathcal{E}_{3}^{k+1} \mathcal{E}_{4}^{k+1} \mathcal{E}_{5}^{k+1} \mathcal{E}_{7}^{k+1} \mathcal{E}_{7}^{k+1}

Figure 1: The parallel LADMM algorithm

As shown in Figure 1, we divide \boldsymbol{X} and \boldsymbol{y} into M row blocks using the following approach,

$$\boldsymbol{y} = (\boldsymbol{y}_1^{\top}, \boldsymbol{y}_2^{\top}, \dots, \boldsymbol{y}_M^{\top})^{\top}, \ \boldsymbol{X} = (\boldsymbol{X}_1^{\top}, \boldsymbol{X}_2^{\top}, \dots, \boldsymbol{X}_M^{\top})^{\top},$$
 (20)

with $X_m \in \mathbb{R}^{n_m \times p}$ and $y_m \in \mathbb{R}^{n_m}$, where $\sum_{m=1}^M n_m = n$. Here, X_m and y_m denote the m-th block of data, which will be processed by the m-th local machine. Correspondingly, r and d can also be divided into M blocks,

$$\boldsymbol{r} = (\boldsymbol{r}_1^{\mathsf{T}}, \boldsymbol{r}_2^{\mathsf{T}}, \dots, \boldsymbol{r}_M^{\mathsf{T}})^{\mathsf{T}}, \ \boldsymbol{d} = (\boldsymbol{d}_1^{\mathsf{T}}, \boldsymbol{d}_2^{\mathsf{T}}, \dots, \boldsymbol{d}_M^{\mathsf{T}})^{\mathsf{T}}.$$
 (21)

Then, we can rewrite problem (14) into the following equivalent problem,

$$\min_{\boldsymbol{\beta}, \boldsymbol{r}_{m}} \sum_{m=1}^{M} \mathcal{L}_{\tau,*}(\boldsymbol{r}_{m}) + P_{\lambda}(|\boldsymbol{\beta}|),$$
s.t. $\boldsymbol{X}_{m}\boldsymbol{\beta} + \boldsymbol{r}_{m} = \boldsymbol{y}_{m}, \ m = 1, 2, \dots, M.$ (22)

Similarly, problem (22) has the following augmented Lagrangian,

$$L_{\mu}(\boldsymbol{\beta}, \boldsymbol{r}_{m}, \boldsymbol{d}_{m}) = \sum_{m=1}^{M} \mathcal{L}_{\tau,*}(\boldsymbol{r}_{m}) + P_{\lambda}(|\boldsymbol{\beta}|) - \sum_{m=1}^{M} \boldsymbol{d}_{m}^{\top}(\boldsymbol{X}_{m}\boldsymbol{\beta} + \boldsymbol{r}_{m} - \boldsymbol{y}_{m}) + \frac{\mu}{2} \sum_{m=1}^{M} \|\boldsymbol{X}_{m}\boldsymbol{\beta} + \boldsymbol{r}_{m} - \boldsymbol{y}_{m}\|_{2}^{2}, \quad (23)$$

where $d_m \in \mathbb{R}^{n_m}$ is the dual variable. Then, the problem (22) can be solved by the following updates.

$$\begin{cases}
\boldsymbol{\beta}^{k+1} = \arg\min_{\boldsymbol{\beta}} \left\{ P_{\lambda}(|\boldsymbol{\beta}|) + \frac{\mu}{2} \sum_{m=1}^{M} \| \boldsymbol{X}_{m} \boldsymbol{\beta} + \boldsymbol{r}_{m}^{k} - \boldsymbol{y}_{m} - \boldsymbol{d}_{m}^{k} / \mu \|_{2}^{2} + \frac{1}{2} \| \boldsymbol{\beta} - \boldsymbol{\beta}^{k} \|_{S}^{2} \right\}, \\
\boldsymbol{r}_{m}^{k+1} = \arg\min_{\boldsymbol{r}_{m}} \left\{ \mathcal{L}_{\tau,*}(\boldsymbol{r}_{m}) + \frac{\mu}{2} \| \boldsymbol{X}_{m} \boldsymbol{\beta}^{k+1} + \boldsymbol{r}_{m} - \boldsymbol{y}_{m} - \boldsymbol{d}_{m}^{k} / \mu \|_{2}^{2} \right\}, m = 1, 2, \dots, M. \\
\boldsymbol{d}_{m}^{k+1} = \boldsymbol{d}_{m}^{k} - \mu (\boldsymbol{X}_{m} \boldsymbol{\beta}^{k+1} + \boldsymbol{r}_{m}^{k+1} - \boldsymbol{y}_{m}), m = 1, 2, \dots, M,
\end{cases} (24)$$

where $\mathbf{S} = \eta \mathbf{I}_p - \mu \sum_{m=1}^{M} \mathbf{X}_m^{\top} \mathbf{X}_m = \eta \mathbf{I}_p - \mu \mathbf{X}^{\top} \mathbf{X}$. Please note that although in theoretical analysis, η can take the same value as the non-parallel version, in practice, each sub-machine only loads a portion of the data, which means we can only obtain $\eta_m = \text{eigen}(\mu \mathbf{X}_m^{\top} \mathbf{X}_m)$. Note also that $\sum_{m=1}^{M} \eta_m \geq \text{eigen}(\mu \mathbf{X}^{\top} \mathbf{X})$. Therefore, in the specific implementation of the parallel algorithm, we can choose $\sum_{m=1}^{M} \eta_m$ as the value for η .

Similar to (19), the iteration of $\boldsymbol{\beta}$ and \boldsymbol{r}_m can be represented as

$$\begin{cases}
\boldsymbol{\beta}^{k+1} = \operatorname{prox}_{\eta, P_{\lambda}} \left(\boldsymbol{\beta}^{k} - \frac{\mu \sum_{m=1}^{M} \boldsymbol{X}_{m}^{\top} (\boldsymbol{X}_{m} \boldsymbol{\beta}^{k} + \boldsymbol{r}_{m}^{k} - \boldsymbol{y}_{m} - \boldsymbol{d}_{m}^{k} / \mu)}{\eta} \right), \\
\boldsymbol{r}_{m}^{k+1} = \operatorname{prox}_{\mu, \mathcal{L}_{\tau, *}} \left(\boldsymbol{y}_{m} + \boldsymbol{d}_{m}^{k} / \mu - \boldsymbol{X}_{m} \boldsymbol{\beta}^{k+1} \right), m = 1, 2, \dots, M.
\end{cases} (25)$$

Then, the iterative scheme of parallel LADMM for (14) can be described in Algorithm 2.

Next, we will describe the relationship between Algorithm 1 and Algorithm 2. For ease of distinction, we set $\left\{\hat{\beta}^k, \hat{r}^k, \hat{d}^k\right\}$ as the result of the k-th iteration of Algorithm 1, and $\left\{\tilde{\beta}^k, \tilde{r}^k, \tilde{d}^k\right\}$ as the result of the k-th iteration of Algorithm 2. Then, we have the following surprising conclusion.

Algorithm 2 Parallel LADMM for solving NPSQR.

Input: Observation data $\{X_m, y_m\}_{m=1}^M$; primal variables $\beta^0, \{r_m^0\}_{m=1}^M$; dual variables $\{d^0\}_{m=1}^M$; augmented parameters μ ; penalty parameter λ_1 and λ_2 ; and selectable parameters $\tau \in (0,1)$ and c or $\kappa > 0$.

Output: The last iteration β^K .

Calculate: $\{\eta_m = \text{eigen}(\mu \boldsymbol{X}_m^{\top} \boldsymbol{X}_m)\}_{m=1}^M \text{ and } \eta = \sum_{m=1}^M \eta_m.$

while not converged do

1. Update $\boldsymbol{\beta}_{j}^{k+1} = \operatorname{prox}_{\eta, P_{\lambda}} \left(\boldsymbol{\beta}_{j}^{k} - \frac{\left(\mu \sum_{m=1}^{M} \boldsymbol{\xi}_{m}^{k}\right)_{j}}{\eta} \right), j = 1, 2, \dots, p,$

2. Update $\boldsymbol{r}_{m_{l}}^{k+1} = \operatorname{prox}_{\mu,\mathcal{L}_{\tau,*}} \left([\boldsymbol{y}_{m} + \boldsymbol{d}_{m}^{k}/\mu - \boldsymbol{X}_{m}^{\prime}\boldsymbol{\beta}^{k+1}]_{l} \right), m = 1, 2, \dots, M, l = 1, 2, \dots, n_{m},$ 3. Update $\boldsymbol{d}_{m}^{k+1} = \boldsymbol{d}_{m}^{k} - \mu(\boldsymbol{X}_{m}\boldsymbol{\beta}^{k+1} + \boldsymbol{r}_{m}^{k+1} - \boldsymbol{y}_{m}), m = 1, 2, \dots, M,$ 4. Calculate $\boldsymbol{\xi}_{m}^{k+1} = \boldsymbol{X}_{m}^{\top}(\boldsymbol{X}_{m}\boldsymbol{\beta}^{k+1} + \boldsymbol{r}_{m}^{k+1} - \boldsymbol{y}_{m} - \boldsymbol{d}_{m}^{k+1}/\mu), m = 1, 2, \dots, M.$

end while

return solution

Theorem 1 Starting from the same initial value, the iterative solutions obtained by these two algorithms are actually the same, i.e.,

$$\left\{\hat{\boldsymbol{\beta}}^{k}, \hat{\boldsymbol{r}}^{k}, \hat{\boldsymbol{d}}^{k}\right\} = \left\{\tilde{\boldsymbol{\beta}}^{k}, \tilde{\boldsymbol{r}}^{k}, \tilde{\boldsymbol{d}}^{k}\right\}, \text{ for all } k.$$
(26)

This theorem asserts that regardless of the number of local machines M and the number of small samples n_m processed by each machine, the solution obtained from the parallel LADMM algorithm remains unchanged and is identical to that of Algorithm 1. Although this conclusion may not be immediately intuitive, the proof for it is surprisingly simple. Looking back at (20) and (21), we have

$$\left[\mu \boldsymbol{X}^{\top} (\boldsymbol{X}\boldsymbol{\beta}^k + \boldsymbol{r}^k - \boldsymbol{y} - \boldsymbol{d}^k/\mu)\right] = \left[\mu \sum_{m=1}^{M} \boldsymbol{X}_m^{\top} (\boldsymbol{X}_m \boldsymbol{\beta}^k + \boldsymbol{r}_m^k - \boldsymbol{y}_m - \boldsymbol{d}_m^k/\mu)\right].$$

If the two algorithms has the same k-th iteration solution $\{\beta^k, r^k, d^k\}$, then we obtain

$$\hat{\boldsymbol{\beta}}^{k+1} = \tilde{\boldsymbol{\beta}}^{k+1}.\tag{27}$$

From (27), we immediately have $\hat{r}^{k+1} = \tilde{r}^{k+1}$ and $\hat{d}^{k+1} = \tilde{d}^{k+1}$. As a result, Theorem 1 is proved.

Assume that $\mathbf{X}^{\top}\mathbf{X} > \mu \mathbf{I}_p$, where $\mu > 0$ is a constant. The assumption is actually the lower restricted eigenvalue condition which is required in many penalized linear models. We now demonstrate the convergence of the LADMM algorithm, and the proof is given in Appendix B.

Theorem 2 Let the sequence $\mathbf{w}^k = \{\boldsymbol{\beta}^k, \mathbf{r}^k, \mathbf{d}^k\}$ be generated by Algorithms 1 or 2 with an arbitrary initial feasible solution $\mathbf{w}^0 = \{\boldsymbol{\beta}^0, \mathbf{r}^0, \mathbf{d}^0\}$. With the conditions $\mu > \frac{\sqrt{2}}{\sqrt{n} \min\{c, \kappa\}}$ and $\eta > eigen(\mu \mathbf{X}^{\top} \mathbf{X})$, then the sequence \mathbf{w}^k converges to $\mathbf{w}^* = \{\boldsymbol{\beta}^*, \mathbf{r}^*, \mathbf{d}^*\}$, where \mathbf{w}^* is a critical point of L_{μ} .

Remark 1 To solve the NPSQR with $\mathcal{L}_{\tau,c}$, the condition $\mu > \frac{\sqrt{2} \max\{\tau, 1-\tau\}}{\sqrt{n}c}$ guarantees convergence of the algorithm. On the other hand, for the NPSQR with $\mathcal{L}_{\tau,\kappa}$, the algorithm can converge as long as $\mu > \frac{\sqrt{2}}{\sqrt{n}\kappa}$. The reason behind the different requirements for μ in these two models lies in the disparity of the Lipschitz constant of the first derivative of the two smooth quantile losses. In the case of large samples (n is large), the condition $\mu > \frac{\sqrt{2}}{\sqrt{n} \min\{c,\kappa\}}$, which ensures convergence, can be easily satisfied.

3.3 Comparison with Other Parallel ADMM Algorithms

While there is currently a lack of parallel algorithms specifically designed for solving the NPSQR problem, there have been recent studies proposing parallel ADMM algorithms for the nonconvex penalized quantile regression (NPQR), such as Yu et al. (2017b), Fan et al. (2020) and Wen et al. (2023). It is worth noting that by disregarding constant terms, we can observe that as the values of c and κ approach 0, the function $\mathcal{L}_{\tau,*}$ converges to the quantile loss. Consequently, our algorithm can also be applied to solve the NPQR problem. To provide a more comprehensive comparison, we reviewed several parallel ADMM algorithms that address the NPQR problem.

• QPADM in Yu et al. (2017b). To have a parallel structure, auxiliary variables $\{\beta_m = \beta\}_{m=1}^M$ are added to (14). This modification transforms the constrained optimization problem into the following form,

$$\min_{\boldsymbol{\beta}, \boldsymbol{r}_m, \boldsymbol{\beta}_m} \sum_{m=1}^{M} \rho_{\tau}(\boldsymbol{r}_m) + P_{\lambda}(|\boldsymbol{\beta}|),$$
s.t. $\boldsymbol{X}_m \boldsymbol{\beta}_m + \boldsymbol{r}_m = \boldsymbol{y}_m, \boldsymbol{\beta}_m = \boldsymbol{\beta}, m = 1, 2, \dots, M.$ (28)

Problem (28) has the following augmented Lagrangian,

$$L_{\mu}(\boldsymbol{\beta}, \boldsymbol{r}_{m}, \boldsymbol{\beta}_{m}, \boldsymbol{d}_{m}) = \sum_{m=1}^{M} \rho_{\tau}(\boldsymbol{r}_{m}) + P_{\lambda}(|\boldsymbol{\beta}|) - \sum_{m=1}^{M} \boldsymbol{d}_{1m}^{\top}(\boldsymbol{X}_{m}\boldsymbol{\beta}_{m} + \boldsymbol{r}_{m} - \boldsymbol{y}_{m})$$
$$+ \frac{\mu}{2} \sum_{m=1}^{M} \|\boldsymbol{X}_{m}\boldsymbol{\beta}_{m} + \boldsymbol{r}_{m} - \boldsymbol{y}_{m}\|_{2}^{2} - \sum_{m=1}^{M} \boldsymbol{d}_{2m}^{\top}(\boldsymbol{\beta}_{m} - \boldsymbol{\beta}) + \frac{\mu}{2} \sum_{m=1}^{M} \|\boldsymbol{\beta}_{m} - \boldsymbol{\beta}\|_{2}^{2},$$
(29)

where $d_{1m} \in \mathbb{R}^{n_m}$ and $d_{2m} \in \mathbb{R}^p$ are the dual variables. The parallel ADMM iterative scheme of (29) is

$$\begin{cases}
\boldsymbol{\beta}^{k+1} = \arg\min_{\boldsymbol{\beta}} \left\{ P_{\lambda}(|\boldsymbol{\beta}|) + \frac{\mu}{2} \sum_{m=1}^{M} \left\| \boldsymbol{\beta}_{m}^{k} - \boldsymbol{\beta} - \boldsymbol{d}_{2m}^{k} / \mu \right\|_{2}^{2} \right\}, \\
\boldsymbol{r}_{m}^{k+1} = \arg\min_{\boldsymbol{r}_{m}} \left\{ \rho_{\tau}(\boldsymbol{r}_{m}) + \frac{\mu}{2} \left\| \boldsymbol{X}_{m} \boldsymbol{\beta}_{m}^{k+1} + \boldsymbol{r}_{m} - \boldsymbol{y}_{m} - \boldsymbol{d}_{1m}^{k} / \mu \right\|_{2}^{2} \right\}, \\
\boldsymbol{\beta}_{m}^{k+1} = \arg\min_{\boldsymbol{\beta}_{m}} \left\{ \left\| \boldsymbol{X}_{m} \boldsymbol{\beta}_{m} + \boldsymbol{r}_{m}^{k} - \boldsymbol{y}_{m} - \boldsymbol{d}_{1m}^{k} / \mu \right\|_{2}^{2} + \left\| \boldsymbol{\beta}_{m} - \boldsymbol{\beta}^{k+1} - \boldsymbol{d}_{2}^{k} / \mu \right\|_{2}^{2} \right\}, \\
\boldsymbol{d}_{1m}^{k+1} = \boldsymbol{d}_{1m}^{k} - \mu (\boldsymbol{X}_{m} \boldsymbol{\beta}_{m}^{k+1} + \boldsymbol{r}_{m}^{k+1} - \boldsymbol{y}_{m}), \\
\boldsymbol{d}_{2m}^{k+1} = \boldsymbol{d}_{2m}^{k} - \mu (\boldsymbol{\beta}_{m}^{k+1} - \boldsymbol{\beta}^{k+1}).
\end{cases} (30)$$

Note that when M=1, the algorithm becomes a nonparallel version of ADMM. It can be observed that by increasing the consensus constraint $\beta_m = \beta$, internal loops are avoided. However, this change also introduces an additional step in solving β_m , which requires finding the inverse of $X_m^{\top}X_m + I_{n_m}$. Although Yu et al. (2017b) suggests using the Woodbury matrix identity to alleviate the computational burden of inverting these matrices, the matrix multiplication can still be time-consuming when p is large. Motivated by the maximization in QICD proposed by Peng and Wang (2015), QPADM transforms nonconvex problems into weighted ℓ_1 soft-shrinkage operator for β subproblems. However, this approximation may result in too many iterative steps.

• QPADMslack in Fan et al. (2020). Inspired by Guan et al. (2018), Fan et al. (2020) relaxed r_m to $u_m - v_m$ with $u_m \geq 0$ and $v_m \geq 0$, and made an improvement in solving the β subproblem. These measures can reduce the iteration steps and improve the computational accuracy of QPADM in calculating NPQR. The constrained optimization problem is

$$\min_{\boldsymbol{\beta}, \boldsymbol{u}_{m}, \boldsymbol{v}_{m}, \boldsymbol{\beta}_{m}} \quad \sum_{m=1}^{M} \left(\tau \boldsymbol{u}_{m} + (1 - \tau) \boldsymbol{v}_{m} \right) + P_{\lambda}(|\boldsymbol{\beta}|),$$
s.t.
$$\boldsymbol{X}_{m} \boldsymbol{\beta}_{m} + \boldsymbol{u}_{m} - \boldsymbol{v}_{m} = \boldsymbol{y}_{m},$$

$$\boldsymbol{\beta}_{m} = \boldsymbol{\beta}, m = 1, 2, \dots, M.$$
(31)

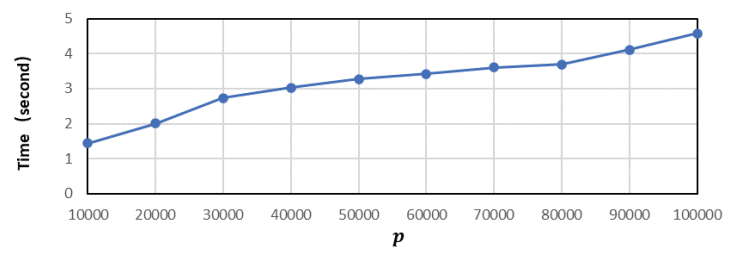
Similar to the steps of QPADM before the iterative process, the only difference is that the r subproblem is replaced by the u and v subproblems. In addition, compared to the approximate solution of β in the QPADM, QPADMslack uses the approximate closed-form solution for SCAD and MCP proposed by Gong et al. (2013) and Guan et al. (2018). The so-called approximate closed-form solution means that it obtains the minimum point by comparing the minimum value of the objective function among several candidate minimum points. In contrast, our LADMM algorithm utilizes the derived proximal operator to directly provide a closed-form for this nonconvex problem.

The above algorithms are all parallel algorithms for samples. The QPADM requires iterating over (2M + 1)p + 2nM variables, while the QPADMslack needs to iterate over (2M + 1)p + 3nM variables. When p is very large, the Woodbury matrix identity that needs to be used is

$$(\boldsymbol{X}_m^{\top} \boldsymbol{X}_m + \boldsymbol{I}_p)^{-1} = \boldsymbol{I}_p - \boldsymbol{X}_m^{\top} (\boldsymbol{X}_m \boldsymbol{X}_m^{\top} + \boldsymbol{I}_{n_m})^{-1} \boldsymbol{X}_m.$$

The matrix multiplication here is quite time-consuming. Our LADMM algorithm only needs to iterate p+2n variables and only needs to compute the maximum eigenvalue of the matrix $X^{T}X$. We use the power method provided by Golub and Loan (1996) to calculate the maximum eigenvalue. This method is very efficient. We illustrate the time required to calculate the maximum eigenvalue as p changes in the following figure. The R code for computing the maximum eigenvalue is also available in our R package.

Figure 2: The time required to compute the maximum eigenvalue of a matrix, with the presented result being the average of 100 repetitions.



• Feature-splitting ADMM in Wen et al. (2023). Inspired by the three-block ADMM in Sun et al. (2015), Wen et al. (2023) propose a feature-splitting algorithm for solving ℓ_1 quantile regression. Furthermore, guided by the theoretical results of Fan et al. (2014), they utilized the LLA algorithm to solve NPQR. Specifically, they used ℓ_1 quantile regression as the initial value and repeated the calculation a few times, achieving a high probability of convergence to the solution

of NPQR. The FSADMM requires iterating over p + (3M - 1)n variables, where M is the number of local machines. Therefore, when n is relatively large, FSADMM may encounter computational difficulties with many local machines.

4 Simulation Studies

In this section, we demonstrate the model selection and estimation accuracy, as well as the computational efficiency of LADMM in nonparallel and/or parallel environments by solving NPQR (Wang et al. (2012)), nonconvex penalized least squares and Huber regression (Fan et al. (2018) and Pan et al. (2021)), and NPSQR (Mkhadri et al. (2017)). Inspired by Lee et al. (2014) and Yu et al. (2017b), we also choose the λ_1 and/or λ_2 that minimize

$$HBIC(\lambda_1, \lambda_2) = \log \left(\sum_{i=1}^n \mathcal{L}(y_i - \boldsymbol{x}_i^{\top} \hat{\boldsymbol{\beta}}_{\lambda_1, \lambda_2}) \right) + |S_{\lambda_1, \lambda_2}| \frac{\log(\log n)}{n} C_n,$$
(32)

where \mathcal{L} is a loss function, and $\hat{\boldsymbol{\beta}}_{\lambda_1,\lambda_2}$ is its corresponding nonconvex estimator. $|S_{\lambda_1,\lambda_2}|$ is the number of nonzero coordinates of $\hat{\boldsymbol{\beta}}_{\lambda_1,\lambda_2}$, and C_n is a sequence of positive constants diverging to infinity as n increases such that $C_n = O(\log p)$.

All experiments were conducted using R on computer with AMD Ryzen 9 7950X 16-Core Processor 4.50 GHz and 32 GB RAM. Additionally, we have implemented the LADMM algorithm in an R package called PIPADMM, which can be accessed at https://github.com/xfwu1016/PIPADMM.

4.1 Simulation for NPQR

The first simulation applies LADMM to solve NPQR and compares its performance with some recent algorithms such as QRADM in Yu et al. (2017b), QRADMslack in Fan et al. (2020), and Feature-splitting ADMM ((FSADMM) in Wen et al. (2023). Both Yu et al. (2017b) and Fan et al. (2020) have provided R packages for computing the respective algorithms, but these packages can only run on Mac. Moreover, the QPADM package can only output estimated parameters and does not provide iteration count and iteration time. In order to ensure fairness in the comparison, we have rewritten the R code for the QPADM algorithm and QPADMslack algorithm on Windows based on their papers. For all the tested ADMM algorithms, the maximum iteration number was

set to be 500 and the stopping criterion was defined as follows,

$$\frac{\|\boldsymbol{\beta}^k - \boldsymbol{\beta}^{k-1}\|_2}{\max(1, \|\boldsymbol{\beta}^k\|_2)} \le 10^{-4}.$$

Like in the simulation studies of Peng and Wang (2015), Yu et al. (2017b), Fan et al. (2020) and Wen et al. (2023), we generate a heteroscedastic regression model with the equation $y = x_6 + x_{12} + x_{15} + x_{20} + 0.7x_1\epsilon$, where $\epsilon \sim N(0,1)$. The covariates $(x_1, x_2, ..., x_p)$ are generated in two steps. First, we generate $\tilde{x} = (\tilde{x}_1, \tilde{x}_2, ..., \tilde{x}_p)^{\top}$ from a p-dimensional multivariate normal distribution $N(\mathbf{0}, \mathbf{\Sigma})$, where $\Sigma_{ij} = 0.5^{|i-j|}$ for $1 \leq i, j \leq p$. Second, we set $x_1 = \Phi(\tilde{x}_1)$ and $x_j = \tilde{x}_j$ for j = 2, ..., p. In nonparallel environments (M = 1), we simulate datasets with sizes (n, p) = (30,000, 1,000), (1,000, 30,000), (10,000, 10,000) and (30,000, 30,000). In parallel environments (M > 1), we simulate datasets with sizes (n, p) = (200,000, 500) and (500,000,1000). Each simulation is repeated 100 times, and the average results for both nonparallel and parallel computations are presented in Table 1 and Table 2, respectively. Due to space limitations, this section will only focus on the results of the SCAD (a=3.7) and $\tau = 0.7$, and the other simulation results are included in the Appendix C.1.

Table 1: Comparison of various ADMMs with SCAD penalty of different data sizes.

(n,p)	(300	00,100	00)			(1000,30000)					
	P1	P2	AE	Ite	Time	P1	P2	AE	Ite	Time	
QPADM	100	100	0.015(0.03)	105.6(12.3)	37.53(6.3)	0	100	7.621(0.84)	500(0.0)	1924.5(55.3)	
QPADMslack	100	100	0.059(0.03)	51.2 (5.7)	35.95(4.5)	0	100	8.465(1.12)	216(13.5)	1133.8(39.4)	
FSADMM	100	100	0.017(0.04)	500(0.0)	155.6(11.3)	100	100	0.621(0.09)	500(0.0)	134.1(10.1)	
LADMM	100	100	0.022(0.03)	44(2.9)	34.53(4.2)	100	100	0.482(0.05)	166(11.9)	60.7(5.0)	
(n,p)	(100	00,300	000)			(300	00,300	000)			
	P1	P2	AE	Ite	Time	P1	P2	AE	Ite	Time	
QPADM	100	100	3.891(1.23)	500(0.0)	2178.4(66.8)	100	100	1.758(0.13)	500(0.0)	3264.3(56.3)	
QPADMslack	100	100	4.171(1.64)	252(20.7)	1429.6(35.7)	100	100	2.263(0.25)	327(21.1)	2126.3(41.2)	
FSADMM	100	100	0.592(0.16)	500(0.0)	238.9(18.1)	100	100	1.092(0.10)	500(0.0)	424.2(17.4)	
I SADMINI	100										

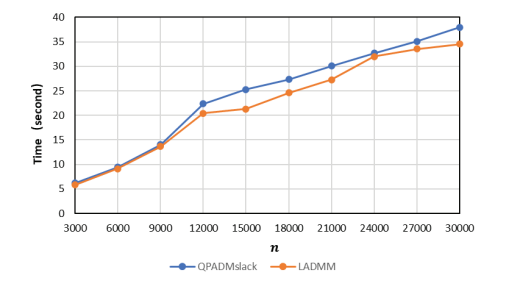
^{*} The meanings of the notations used in this table are as follows: P1 (%): proportion that x_1 is selected; P2 (%): proportion that x_6 , x_{12} , x_{15} , and x_{20} are selected; AE: absolute estimation error; Ite: number of iterations; Time (s): running time. Numbers in the parentheses represent the corresponding standard deviations. The optimal solution is represented in bold.

Table 2: Comparison of various parallel ADMMs with SCAD penalty.

	QPADM		(2	00000, 500)	QPADM		(5	00000, 1000)
Μ	Nonzero	AE	Ite	Time	Nonzero	AE	Ite	Time
5 20 100	35.3(1.8) 38.4(2.0) 40.6(2.3)	0.053(0.0008) 0.068(0.0011) 0.085(0.0025)	342.8(23.9) 375.1(29.2) 419.7(67.8)	72.8(5.6) 39.8(4.7) 18.6(3.3)	25.7(1.3) 27.4(1.7) 33.5(2.1)	$0.043(0.0007) \\ 0.051(0.0009) \\ 0.077(0.0018)$	458.3(35.8) 483.1(39.2) 496.7(17.8)	182.8(10.5) 99.5(5.9) 38.6(4.7)
	QPADMs	lack	(2	00000, 500)	QPADMs	lack	(5	00000, 1000)
Μ	Nonzero	AE	Ite	Time	Nonzero	AE	Ite	Time
5 20 100	34.6(1.9) 39.7(2.1) 41.2(2.5)	$0.062(0.0017) \\ 0.075(0.0024) \\ 0.094(0.0031)$	214.4(25.4) 236.3(26.9) 375.7(82.6)	31.2(4.0) 10.7(2.1) 4.6(0.8)	24.9(1.2) 29.5(1.5) 32.3(1.9)	0.039(0.0006) 0.048(0.0010) 0.074(0.0021)	311.7(28.3) 347.3(32.5) 396.5(72.3)	79.5(7.3) 41.2(5.5) 20.9(2.4)
	LADMM		(2	00000, 500)	LADMM		(5	00000, 1000)
M	Nonzero	AE	Ite	Time	Nonzero	AE	Ite	Time
5 20 100	5.6(0.4) 5.6(0.4) 5.6(0.4)	0.055(0.0008) 0.055(0.0008) 0.055(0.0008)	49.7(1.2) 49.7(1.2) 49.7(1.2)	19.7(1.0) 10.3(0.7) 5.3(0.4)	5.4(0.3) $5.4(0.3)$ $5.4(0.3)$	$\begin{array}{c} 0.032 (0.0005) \\ 0.032 (0.0005) \\ 0.032 (0.0005) \end{array}$	78.7(3.4) $78.7(3.4)$ $78.7(3.4)$	32.6(2.3) $20.5(1.8)$ $15.5(1.2)$

^{*} P1 and P2 are not presented in Table 2 because all methods have a value of 100 for these two metrics. Theorem 1 ensures that the Nonzero, AE, and Ite of LADMM are not affected by the M value.

Table 1 demonstrates that LADMM outperforms QPADM and QPADMslack in terms of computational speed and estimation accuracy when the dimensionality of the problem p is large. LADMM also outperforms FSADMM when the sample size n is large. We further demonstrate the advantages of proposed LADMM in terms of time in Figure 3. Notably, for scenarios where both n and p are large, LADMM demonstrates remarkable advantages in terms of computational efficiency and accuracy compared to other ADMM algorithms. Table 2 illustrates that when multiple local machines are employed, LADMM showcases comparable performances in terms of computational time and accuracy compared to QRADM and QRADMslack. We visualize this result in Figure 4.



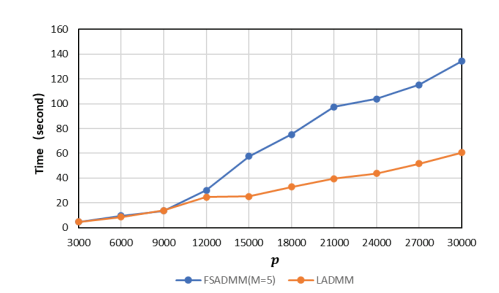
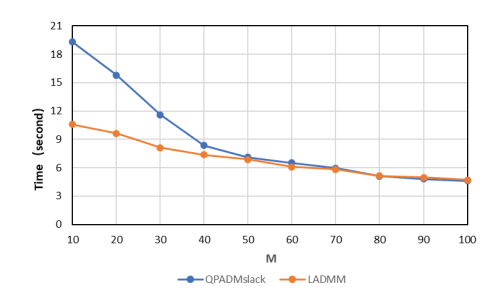


Figure 3: Time comparison of LADMM, QPADMslack and FSADMM. On the left, the dimension of the data is p = 500; On the right, the sample size of the data is n = 500.



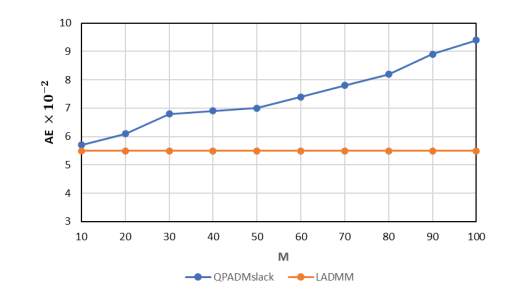


Figure 4: Computational time and absolute error (AE) of QPADMslack and LADMM with n = 400000, p = 1000.

Table 3: Comparison of LS-SCAD and Huber-SCAD Calculated by LADMM and ILAMM

		LS-S	SCAD			Huber-SCAD			
(n,p)	Algorithm	FP	FN	AE	Time	FP	FN	AE	Time
(100,1000)	ILAMM	0	1	0.34(0.08)	8.8(1.1)	0	1	0.41(0.07)	23.2(5.2)
(100,1000)	LADMM	0	0	0.29(0.07)	1.3(0.2)	0	0	0.34(0.07)	1.41(0.3)
(100 10000)	ILAMM	0	0	0.50(0.10)	175.3(10.3)	0	0	0.52(0.18)	362.9(15.9)
(100,10000)	LADMM	0	0	0.41(0.09)	7.1(1.0)	0	0	0.49(0.16)	7.8(0.8)
(10000 10000)	ILAMM	0	1	0.05(0.01)	1885(121.4)	0	1	0.07(0.01)	2314(102.3)
(10000,10000)	LADMM	0	0	0.06(0.02)	31.38(6.7)	0	0	0.01(0.00)	35.26(7.5)

^{*} False Positive (FP) refers to the number of variables with a coefficient of zero that are mistakenly included in the final model, while False Negative (FN) refers to the number of variables with non-zero coefficients that are omitted from the model.

4.2 Simulation for NPLS and NPHR

In this simulation, we utilize the proposed LADMM method and the ILAMM algorithm proposed in Fan et al. (2018) and Pan et al. (2021) to solve nonconvex penalized least squares regression (NPLS) and nonconvex penalized Huber regression (NPHR). We then compare the performance of these methods. Pan et al. (2021) provided a R package for ILAMM algorithm which is available at https://github.com/XiaoouPan/ILAMM. Similar to Pan et al. (2021), we generate the heteroscedastic model, $y_i = \boldsymbol{x}_i^{\mathsf{T}}\boldsymbol{\beta} + c^{-1}(\boldsymbol{x}_i^{\mathsf{T}}\boldsymbol{\beta})^2 \epsilon_i$ with $\boldsymbol{x}_i \sim N(\mathbf{0}, \boldsymbol{I}_p)$ for $i = 1, \ldots, n$, where the constant c is chosen as $c = \sqrt{3}\boldsymbol{\beta}^{\mathsf{T}}\boldsymbol{\beta}$ such that $E\left(c^{-1}(\boldsymbol{x}_i^{\mathsf{T}}\boldsymbol{\beta})^2\right)^2 = 1$. The true vector of regression coefficients $\boldsymbol{\beta}$ is $(4,3,2,-2,-2,-2,0,\ldots,0)^{\mathsf{T}}$. Moreover, we consider the following two error distributions.

- Normal distribution: $\epsilon_i \sim N(\mu, \sigma^2)$ with $\mu = 0$ and standard deviation $\sigma = 1.5$.
- Lognormal distribution: $\epsilon_i \sim LN(\mu, \sigma^2)$ with $\mu = 0$ and $\sigma = 1.2$.

Table 3 presents the simulation results of LADMM and ILAMM solving least squares SCAD

(LS-SCAD) and Huber SCAD models (Huber-SCAD) when the errors follow a normal distribution. The simulation results for the Lognormal distribution, as well as other nonconvex penalties, are presented in the Appendix C.2. Each result in the table represents the mean value of 100 repeated experiments, and the standard deviation is denoted in parentheses. The results presented in Table 3 demonstrate that LADMM outperforms the ILAMM in effectively solving both NPLS and NPHR models. In addition, if p is large, ILAMM may be time-consuming.

4.3 Simulation for NPSQR

In this example, we utilize the proposed LADMM and Mkhadri et al. (2017) method to solve nonconvex penalized smooth quantile regression (NPSQR) and compare their performances. Mkhadri et al. (2017) provided an efficient R package for calculating NPSQR, which can be found at the following https://github.com/KarimOualkacha/cdaSQR/tree/master. Following the scenario 3 in Section 4.2 of Mkhadri et al. (2017), we generate the data sets with $y_i = \mathbf{x}_i^{\mathsf{T}} \boldsymbol{\beta} + \epsilon_i$, where $\epsilon \sim N(0, \sigma^2 \mathbf{I}_p)$ and $\sigma = 5$. The covariates (x_1, x_2, \dots, x_p) are generated from $N(\mathbf{0}, \mathbf{\Sigma})$, where $\Sigma_{ij} = 0.5^{|i-j|}$ for $1 \leq i, j \leq p$. The true vector of regression coefficients is

$$\boldsymbol{\beta} = (\underbrace{3, \dots, 3}_{5}, \underbrace{-1.5, \dots, -1.5}_{5}, \underbrace{1, \dots, 1}_{5}, \underbrace{2, \dots, 2}_{5}, \underbrace{0, \dots, 0}_{p-20})^{\top}$$

The comparison results of our algorithm LADMM with cdaSQR are summarized in Table 4. These results are all about Snet, and the results for Mnet and Cnet are in the Appendix C.3. In terms of computational accuracy and speed, LADMM and cdaSQR perform similarly, but in terms of FP and FN, LADMM has significant advantages.

Table 4: Comparison of LADMM and cdaSQR with $\delta = 0.5$ and $\tau = 0.5$

		cdaS	QR			LAI	OMM		
(n,p)	Loss function	FP	FN	AE	Time	FP	FN	AE	Time
(5000,500)	$\mathcal{L}_{ au,c}$	2.52	7.39	0.47(0.05)	3.36(0.36)	0	0.11	0.34(0.03)	3.62(0.37)
(5000,500)	$\mathcal{L}_{\tau,\kappa}$	3.25	8.36	0.35(0.04)	3.47(0.42)	0	0.08	0.29(0.02)	3.78(0.38)
(10000 1000)	$\mathcal{L}_{ au,c}$	3.98	10.36	1.38(0.08)	5.11(0.82)	0	0.01	0.88(0.05)	4.71(0.67)
(10000,1000)	$\mathcal{L}_{\tau,\kappa}$	2.52	9.47	1.22(0.08)	4.76(0.71)	0	0.04	0.74(0.04)	4.83(0.69)
(20000 2000)	$\mathcal{L}_{ au,c}$	3.69	15.36	1.89(0.12)	24.33(2.39)	0	0.01	0.96(0.09)	20.39(2.48)
(20000,2000)	$\mathcal{L}_{\tau,\kappa}$	4.40	14.77	1.73(0.10)	19.25(2.11)	0	0.05	0.89(0.08)	19.64(2.36)

5 Real Data Studies

In this section, we compare the performance of several parallel ADMM algorithms in an online publicly available dataset, which is available at http://archive.ics.uci.edu/ml/datasets/Online+News+Popus
This dataset provides a summary of the popularity, measured in terms of shares, as well as 60 features of 39,644 news published by Mashable over a two-year period. The features include various aspects such as binary variables indicating news categories (Lifestyle, Entertainment, Business, Social Media, Technology, or World), published time (day of the week and weekend or not), average word length, number of keywords, rate of nonstop words, and more. For more information about the dataset, please refer to the study conducted by Fernandes, Vinagre, and Cortez (2015).

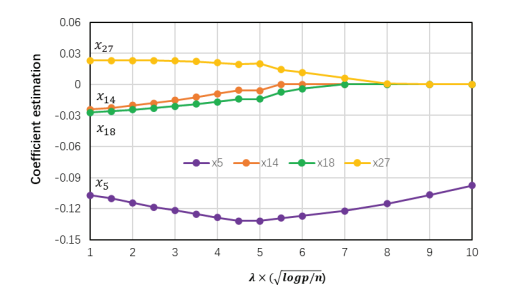
This dataset is heterogeneous in nature, and it has been analyzed by Fan et al. (2020) using NPQR. Their aim is to analyze how various features impact the popularity of news, particularly those that have gained high levels of popularity. They have identified x_{14} (Entertainment) and x_{27} (number of key words) as the two most influential features. However, the empirical results in Fan et al. (2020) also indicated that the QPADM and QPADMslack algorithms tend to select a relatively larger number of variables, and this tendency becomes more pronounced as M increases. The following empirical results will indicate that LADMM does not select so many variables and also has good prediction accuracy.

As in the study of Fan et al. (2020), we standardized the nonbinary factors by zero-mean and unit variance. The features and response variables were denoted as $x_1, x_2, ..., x_{60}$ and y, respectively. To assess the performance of the algorithm, we randomly partitioned the complete dataset 100 times. Each partition consisted of randomly selecting 35,000 samples as the training set, with the remaining samples designated as the test set. To replicate the scenario of parallel computing, we randomly divided the training set into subsets of equal size, with M=10 and M=100 considered in our analysis. We then recorded the average number of selected nonzero coefficients (Nonzero), the prediction error (PE), the number of iterations (Ite), and the running time (Time) of the algorithms. The prediction error (PE) is calculated as follows: $PE = \frac{1}{n_{test}} \sum_{i=1}^{n_{test}} |y_i - \hat{y}_i|$, where $n_{test} = 4644$ represents the sample size of the test set. We only include the results of SCAD in Table 5, and the results of MCP are included in the Appendix C.4.

Table 5: Analysis of the news popularity data under the SCAD penalty with $\tau = 0.5$.

Algorithm	Μ	x_{14}	x_{27}	Nonzero	PE	Ite	Time
QRADM	10	-0.021(0.002)	0.054(0.002)	34.53(1.47)	0.22(0.02)	223.6(37.8)	20.1(2.32)
QNADM	100	-0.020(0.002)	0.056(0.001)	34.82(1.25)	0.20(0.02)	294.8(50.3)	4.5(0.67)
QRADMslack	10	-0.019(0.001)	0.055(0.001)	33.92(1.59)	0.20(0.03)	112.9(11.2)	9.8(1.03)
QRADMSIack	100	-0.018(0.001)	0.057(0.001)	34.07(1.41)	0.20(0.02)	135.4(15.7)	2.1(0.31)
$LADMM_{\varrho}$	10	-0.010(0.001)	0.021(0.001)	10.34(0.56)	0.18(0.02)	81.2(8.4)	3.2(0.21)
$LADMM_{ ho}$	100	-0.010(0.001)	0.021(0.001)	10.34(0.56)	0.18(0.02)	81.2(8.4)	2.2(0.11)
LADMM	10	-0.012(0.001)	0.023(0.001)	12.67(1.35)	0.19(0.01)	65.9(9.6)	2.9(0.13)
$LADMM_{\mathcal{L}_{\tau,c},\delta=1}$	100	-0.012(0.001)	0.023(0.001)	12.67(1.35)	0.19(0.01)	65.9(9.6)	2.1(0.05)
LADMM	10	-0.011(0.001)	0.024(0.001)	13.11(1.45)	0.20(0.01)	72.6(10.1)	3.0(0.21)
$LADMM_{\mathcal{L}_{\tau,\kappa},\delta=1}$	100	-0.011(0.001)	0.024(0.001)	13.11(1.45)	0.20(0.01)	72.6(10.1)	2.1(0.08)

Table 5 demonstrates that the LADMM algorithm exhibit competitive performance in terms of both time and accuracy compared to the QPADM and QPADMslack algorithms. Additionally, LADMM clearly exhibits superior variable selection capability and is not affected by the M value. It is worth noting that, in addition to the important variables x_{14} and x_{27} identified in the previous study, our analysis reveals that variables x_5 (number of stopwords) and x_{18} (a binary variable that represents whether the data channel is the word "world" or not) are also significant. In particular, variable x_5 exhibits a notable importance. We visualize this result using Figure 5. Our newly discovered features are interpretable in real life. Excessive stopwords can make news verbose, trivial and lack coherence, making it difficult to convey clear ideas and information. On the other hand, the use of "world" as data channels for news may result in a relatively smaller audience and, consequently, lower sharing volume, as the focus of news coverage might differ from the interests of the general public.



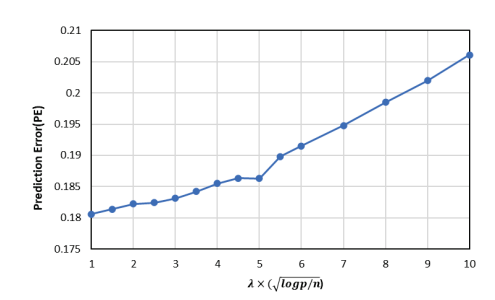


Figure 5: Variation of significance coefficient and prediction error (PE) with λ

6 Conclusion

In this paper, we present a parallel LADMM algorithm for efficiently solving nonconvex penalized smooth quantile regression problems. Our algorithm is easy to implement and offers great flexibility, allowing for its extension to many other nonconvex models such as quantile regression, least squares regression, and Huber regression. Notably, compared to existing parallel algorithms that rely on consensus-based approaches for solving regression models, our solution is not affected by the local machine count and requires fewer iterations for convergence. Furthermore, for smooth loss functions, we prove the global convergence of our LADMM algorithm, meaning that the iterative solutions converge to critical points of the Lagrangian functions.

Our findings demonstrate not only the direct applicability of the LADMM algorithm proposed in this paper to parallel frameworks, but also show that other linearized ADMM algorithms, such as Li et al. (2014) and Gu et al. (2017), can be easily adapted to parallel computation using our strategy. In addition, there is still a lot of work to be studied, such as the convergence of parallel ADMM algorithms for solving NPQR, which has always been an unresolved open problem in Yu et al. (2017b). This paper only uses NPSQR to approximate NPQR, seemingly solving the issue of convergence. However, it has been proven in this study that the global convergence claimed by the Theorem 2 is not guaranteed for arbitrarily small c and κ . In addition, for Huber loss SVM in Wang et al. (2008) and least squares loss SVM in Huang et al. (2014), they also have the property that the loss function is smooth. It is our further work to develop a parallel LADMM algorithm to calculate these classification methods.

Acknowledgements

We are grateful to Professor Karim Oualkacha from the Department of Mathematics at the Université du Québec à Montréal for providing us with the code for the R package cdaSQR. Specifically, we are very grateful to Professor Bingsheng He for his valuable discussions with us, which greatly helped us prove the convergence of the algorithm. The research was supported by the National Natural Science Foundation of China [grant numbers 11871121, 12271066].

References

- Aravkin, A., Kambadur, A., Lozano, A. C. and Luss, R. (2014). Sparse Quantile Huber Regression for Efficient and Robust Estimation[J]. *ArXiv*,1402.4624v1.
- Boyd, S., Parikh, N., Chu, E., Peleato, B. and Eckstein, J. (2010). Distributed Optimization and Statistical Learning via the Alternating Direction Method of Multipliers[J]. Foundations and Trends in Machine Learning, 3(1), 1-122.
- Fan, J. Q., and Li, R. Z. (2001) Variable Selection via Nonconcave Penalized Likelihood and Its Oracle Properties[J]. *Journal of the American Statistical Association*, 96, 1348–1360.
- Fan, J. Q., Liu, H., Sun, Q. and Zhang, T. (2018). I-LAMM for Sparse Learning: Simultaneous Control of Algorithmic Complexity and Statistical Error[J]. *Annals of Statistics*, 46(2), 814-841.
- Fan, Y., Lin, N. and Yin, X. J. (2020). Penalized Quantile Regression for Distributed Big Data Using the Slack Variable Representation[J]. *Journal of Computational and Graphical Statistics*, 30(3), 557-565.
- Fan, J. Q., Xue, L. G. and Zou, H. (2014). Strong Oracle Optimality of Folded Concave Penalized Estimation[J]. *Annals of Statistics*, 819–849.
- Fernandes, K., Vinagre, P., and Cortez, P. (2015). A Proactive Intelligent Decision Support System for Predicting the Popularity of Online News[C]. In Proceedings of the Portuguese Conference on Artificial Intelligence, 535–546.
- Golub, G. H. and Loan, C. (1996). Matrix Computations[M]. The third edition, Johns Hopkins University Press, New York.
- Gong, P. H., Zhang, C. S., Lu, Z. S., Huang, J. Z. and Ye, J. P. (2013). A General Iterative Shrinkage and Thresholding Algorithm for Non-convex Regularized Optimization Problems[C]. *International Conference on Machine Learning*, 28(2), 37–45.
- Guo K., Han D. R. and Wu T. T. (2017). Convergence of Alternating Direction Method for Minimizing Sum of Two Nonconvex Functions with Linear Constraints[J]. *International Journal of Computer Mathematics*, 94(8),1653-1669.
- Gu, Y. W., Fan, J., Kong, L. C., Ma, S. Q. and Zou, H. (2017). ADMM for High-Dimensional Sparse Penalized Quantile Regression[J]. *Technometrics*, 60(3), 319-333.

- Guan, L., Qiao, L., Li, D., Sun, T., Ge, K., and Lu, X. (2018). An Efficient ADMM-Based Algorithm to Nonconvex Penalized Support Vector Machines [C]. In Proceedings of the 2018 IEEE International Conference on Data Mining Workshops, 1209–1216.
- Hee-Seok, Oh., Thomas, C. M. Lee and Douglas, W. Nychka (2011). Fast Nonparametric Quantile Regression With Arbitrary Smoothing Methods[J]. *Journal of Computational and Graphical Statistics*, 20(2), 510-526.
- Huang, J., Breheny, P., Lee, S., Ma, S. and Zhang, C. H. (2016). The Mnet Method for Variable Selection[J]. Statistica Sinica, (3), 903-923.
- Huang, X. L., Shi, L. and Suykens, J. (2014). Asymmetric Least Squares Support Vector Machine Classifiers [J]. Computational Statistics & Data Analysis, 70, 395-405.
- Huber, P. J. (1964). Robust Estimation of a Location Parameter[J]. Annals of Mathematical Statistics, 35(1), 73-101.
- Jennings, L. S., Wong, K. H. and Teo, K. L. (1993). An Optimal Control Problem in Biomechanics[J]. *IFAC Proceedings Volumes*, 26(2), 279-282.
- Kim, J. and Oh, H. S. (2020). Pseudo-quantile Functional Data Clustering[J]. *Journal of Multivariate Analysis*, 178, 104626.
- Koenker, R. and Basset, G. (1970) Regression Quantiles[J]. Econometrica, 46, 33–50
- Lee, E. R., Noh, H., and Park, B. U. (2014). Model Selection via Bayesian Information Criterion for Quantile Regression Models[J]. *Journal of the American Statistical Association*, 109, 216–229.
- Li, G., Peng, H. and Zhu, L. (2011). Nonconcave Penalized M-estimation with a Diverging Number of Parameters[J]. *Statistica Sinica*, 21(1), 391-419.
- Li, X. X., Mo, L. L., Yuan, X. M. and Zhang, J. Z. (2014). Linearized Alternating Direction Method of Multipliers for Sparse Group and Fused LASSO Models[J]. *Computational Statistics & Data Analysis*, 79, 203-221.
- Lin, Z. C., Fang, C. and Li, H. (2022). Alternating Direction Method of Multipliers for Machine Learning [M]. Springer Singapore.

- Mkhadri, A., Ouhourane, M. and Oualkacha, K. (2017). A Coordinate Descent Algorithm for Computing Penalized Smooth Quantile Regression[J]. *Statistics and Computing*, 27, 865–883.
- Negahban, S. N., Ravikumar, P., Wainwright, M. J. and Yu, B. (2010). A Unified Framework for High-dimensional Analysis of M-estimators with Decomposable Regularizers[J]. *Statistical Science*, 27(4), 538-557.
- Newey, W. and Powell, J. (1987). Asymmetric Least Squares Estimation and Testing[J]. *Econometrica*,55 (4), 819–847.
- Ouhourane, M., Yang, Y., Andréa L. Benedet and Oualkacha, K. (2022). Group Penalized Quantile Regression[J]. Statistical Methods and Applications, 31(3), 495-529.
- Pan, X., Sun, Q., and Zhou, W. (2021). Iteratively Reweighted L1-penalized Robust Regression[J]. *Electronic Journal of Statistics*, 3287–3348.
- Peng, B., and Wang, L. (2015). An Iterative Coordinate Descent Algorithm for High-Dimensional Nonconvex Penalized Quantile Regression[J]. *Journal of Computational and Graphical Statistics*, 64, 676–694.
- Loh, P. L. and Wainwright, M. J. (2015). Regularized M-estimators with Nonconvexity: Statistical and Algorithmic Theory for Local Optima[J]. *Journal of Machine Learning Research*.
- Loh, P. L. (2017). Statistical Consistency and Asymptotic Normality for High-Dimensional Robust M-Estimators[J]. *Annals of Statistics*, 45, 866–896.
- Sun, D., Toh, K. C. and Yang, L. (2015). A Convergent 3-block Semiproximal Alternating Direction Method of Multipliers for Conic Programming with 4-type Constraints[J]. SIAM Journal on Optimization, 25(2), 882-915.
- Wang, L., Zhu, J. and Zou, H. (2008). Hybrid Huberized Support Vector Machines for Microarray Classification and Gene Selection[J]. *Bioinformatics*, 24(3), 412-419.
- Wang, L., Wu, Y. C. and Li, R. Z. (2012). Quantile Regression for Analyzing Heterogeneity in Ultra-High Dimension[J]. *Journal of the American Statistical Association*, 107, 214-222.
- Wang, X. F. and Yuan, X. M. (2012). The Linearized Alternating Direction Method for Dantzig Selector [J]. SIAM Journal on Scientific Computing, 34(5), 2792-2811.

- Wang, X. M., Park, T. and Carriere, K. C. (2010). Variable Selection via Combined Penalization for High-dimensional Data Analysis[J]. Computational Statistics and Data Analysis, 54(10), 2230-2243.
- Wen, J., Yang, S., Christina, D. W., Jiang, Y. and Li, R. (2023). Feature-splitting Algorithms for Ultrahigh Dimensional Quantile Regression[J]. *Journal of Econometrics*, 2023, 105426.
- Yu, L., and Lin, N. (2017). ADMM for Penalized Quantile Regression in Big Data[J]. *International Statistical Review*, 85, 494–518.
- Yu, L., Lin, N., and Wang, L. (2017). A Parallel Algorithm for Large-Scale Nonconvex Penalized Quantile Regression[J]. *Journal of Computational and Graphical Statistics*, 26, 935–939.
- Zhang, C. H. (2010), Nearly Unbiased Variable Selection Under Minimax Concave Penalty[J]. *Annals of Statistics*, 38, 894–942.
- Zhang, T. (2010) Analysis of Multi-stage Convex Relaxation for Sparse Regularization[J]. *Journal of Machine Learning Research*, 1081-1107.
- Zheng, S. (2011). Gradient Descent Algorithms for Quantile Regression with Smooth Approximation[J]. International Journal of Machine Learning and Cybernetics, 2, 191–207.
- Zhou, W. X., Bose, K., Fan, J. and Liu, H. (2018). A New Perspective on Robust M-estimation: Finite Sample Theory and Applications to Dependence-adjusted Multiple Testing[J]. *Annals of Statistics*, 46(5), 1904–1931.
- Zou, H. and Hastie, T. (2005). Regularization and Variable Selection via the Elastic Net[J]. *Journal of the Royal Statistical Society, Series B (Statistical Methodology)*, 67(2), 301-320.
- Zou, H., and Li, R. Z. (2008). One-step Sparse Estimates in Nonconcave Penalized Likelihood Models[J]. Annals of Statistics, 36(4), 1509-1533.

Appendix

In this file, we first provide the derivation of the closed-form solution for the proximal operator in Section 2.3 of the main text. Next, we give the proof of convergence conclusion in Theorem 2. Finally, we present supplementary numerical experiments.

A Proof of the Closed-form Solution of Proximal Operator

A.1 Loss Fuction

By recalling that the loss function $\frac{1}{n}\mathcal{L}_{\tau,*}(\boldsymbol{u}) = \frac{1}{n}\sum_{i=1}^{n}\mathcal{L}_{\tau,*}(u_i)$, we can divide the optimization problem

$$\underset{\boldsymbol{u}}{\operatorname{arg\,min}} \left\{ \frac{1}{n} \mathcal{L}_{\tau,*}(\boldsymbol{u}) + \frac{\mu}{2} \|\boldsymbol{u} - \boldsymbol{v}\|_{2}^{2} \right\}$$
(33)

into n independent univariate problems, which can be expressed as $\min_{u_i} \left\{ \mathcal{L}_{\tau,*}(u_i) + \frac{\mu}{2} (u_j - v_j)_2^2 \right\}, i = 1, 2, \dots, n$. We denote the minimum solution of (33) by $\hat{\boldsymbol{u}}$.

• $\mathcal{L}_{\tau,c}(u)$: Racalling

$$\mathcal{L}_{\tau,c}(u) = \begin{cases}
\tau(u - 0.5c) & \text{if } u \ge c, \\
\frac{\tau u^2}{2c} & \text{if } u \in [0, c), \\
\frac{(1-\tau)u^2}{2c} & \text{if } u \in [-c, 0), \\
(\tau - 1)(u + 0.5c) & \text{if } u < -c,
\end{cases} \tag{34}$$

Within the domain, it is either a linear or quadratic function. Therefore, it has a closed-form solution in each small domain. After some algebra, we have

$$\hat{\boldsymbol{u}}_{j} = \begin{cases}
\boldsymbol{v}_{j} - \frac{\tau}{n\mu}, & \text{if } \boldsymbol{v}_{j} \geq c + \frac{\tau}{n\mu} \\
\frac{nc\mu\boldsymbol{v}_{j}}{nc\mu+\tau}, & \text{if } 0 \leq \boldsymbol{v}_{j} < c + \frac{\tau}{n\mu} \\
\frac{nc\mu\boldsymbol{v}_{j}}{nc\mu+1-\tau}, & \text{if } -c + \frac{\tau-1}{n\mu} \leq \boldsymbol{v}_{j} < 0 \\
\boldsymbol{v}_{j} - \frac{\tau-1}{n\mu}, & \text{if } \boldsymbol{v}_{j} < -c + \frac{\tau-1}{n\mu}
\end{cases}$$
(35)

• $\mathcal{L}_{\tau,\kappa}(u)$: Racalling

$$\mathcal{L}_{\tau,\kappa}(u) = \begin{cases}
\tau(u - \frac{\tau\kappa}{2}) & \text{if } u > \tau\kappa, \\
\frac{u^2}{2\kappa} & \text{if } u \in [(\tau - 1)\kappa, \tau\kappa], \\
(\tau - 1)[u - \frac{(\tau - 1)\kappa}{2}] & \text{if } u < (\tau - 1)\kappa,
\end{cases}$$
(36)

Similarly, we have

$$\hat{\boldsymbol{u}}_{j} = \begin{cases} \boldsymbol{v}_{j} - \frac{\tau}{n\mu}, & \text{if } \boldsymbol{v}_{j} \geq \tau\kappa + \frac{\tau}{n\mu} \\ \frac{nc\mu\boldsymbol{v}_{j}}{nc\mu+\tau}, & \text{if } (\tau-1)\kappa + \frac{\tau-1}{n\mu} \leq \boldsymbol{v}_{j} < \tau\kappa + \frac{\tau}{n\mu} \\ \boldsymbol{v}_{j} - \frac{\tau-1}{n\mu}, & \text{if } \boldsymbol{v}_{j} < (\tau-1)\kappa + \frac{\tau-1}{n\mu} \end{cases}$$
(37)

A.2 Nonconvex Penalty

By recalling that the nonconvex penalty $P_{\lambda}(|u|) = \sum_{j=1}^{p} P_{\lambda}(|u_{j}|)$, we can divide the optimization problem

$$\underset{\boldsymbol{u}}{\operatorname{arg\,min}} \left\{ P_{\lambda}(|\boldsymbol{u}|) + \frac{\eta}{2} \|\boldsymbol{u} - \boldsymbol{v}\|_{2}^{2} \right\}$$

into p independent univariate problems, which can be expressed as $\min_{u_j} \left\{ P_{\lambda}(|u_j|) + \frac{\mu}{2} (u_j - v_j)_2^2 \right\}, j = 1, 2, \dots, p$. Let

$$\hat{u}_j \in \underset{u_j}{\operatorname{arg\,min}} \left\{ P_{\lambda}(|u_j|) + \frac{\eta}{2} (u_j - v_j)_2^2 \right\},$$
 (38)

we have $\operatorname{sign}(\hat{u}_j) = \operatorname{sign}(v_j)$ and $\operatorname{sign}(v_j)\hat{u}_j \geq 0$. Let $\tilde{u}_j = \operatorname{sign}(v_j)\hat{u}_j$, then

$$\tilde{u}_j \in \underset{u_j>0}{\operatorname{arg\,min}} \left\{ P_{\lambda}(u_j) + \frac{\eta}{2} \left(u_j - |v_j| \right)_2^2 \right\}.$$
 (39)

From (39), we obtain

$$\tilde{u}_j = |v_j| - \nabla P_\lambda(\tilde{u}_j)/\eta \tag{40}$$

This equation plays a **crucial role** in deriving closed-form solutions for the proximal operator of the (nonconvex) penalty term. The solution of this equation is the solution of the operator.

• For Snet, we have

$$\nabla P_{\lambda}(\tilde{u}_{j}) = \begin{cases}
\lambda_{1} + \lambda_{2}\tilde{u}_{j}, & \text{if } \tilde{u}_{j} \leq \lambda_{1}, \\
\frac{a\lambda_{1} - \tilde{u}_{j}}{a - 1} + \lambda_{2}\tilde{u}_{j}, & \text{if } \lambda_{1} < \tilde{u}_{j} < a\lambda_{1}, \\
\lambda_{2}\tilde{u}_{j}, & \text{if } \tilde{u}_{j} \geq a\lambda_{1}.
\end{cases} \tag{41}$$

For $\tilde{u}_j \leq \lambda_1$, the solution of equation (40) is $\frac{\eta |v_j| - \lambda_1}{\eta + \lambda_2}$. For $\lambda_1 < \tilde{u}_j < a\lambda_1$, the solution of equation (40) is $\frac{(a-1)\eta |v_j| - a\lambda_1}{(a-1)(\eta + \lambda_2) - 1}$. For $\tilde{u}_j \geq a\lambda_1$, the solution of equation (40) is $\frac{\eta v_j}{\eta + \lambda_2}$. Together with $\tilde{u}_j > 0$, $\hat{u}_j = \text{sign}(v_j)$, and $(a-1)(\eta + \lambda_2) > 1$, then we have

$$\hat{u}_{j} = \begin{cases} \operatorname{sign}(\boldsymbol{v}_{j}) \cdot \left[\frac{\eta |\boldsymbol{v}_{j}| - \lambda_{1}}{\eta + \lambda_{2}} \right]_{+}, & \text{if } |\boldsymbol{v}_{j}| \leq \frac{\lambda_{1}(1 + \eta + \lambda_{2})}{\eta} \\ \operatorname{sign}(\boldsymbol{v}_{j}) \cdot \left[\frac{(a - 1)\eta |\boldsymbol{v}_{j}| - a\lambda_{1}}{(a - 1)(\eta + \lambda_{2}) - 1} \right]_{+}, & \text{if } \frac{\lambda_{1}(1 + \eta + \lambda_{2})}{\eta} < |\boldsymbol{v}_{j}| < \frac{a\lambda_{1}(\eta + \lambda_{2})}{\eta} \\ \frac{\eta \boldsymbol{v}_{j}}{\eta + \lambda_{2}}, & \text{if } |\boldsymbol{v}_{j}| \geq \frac{a\lambda_{1}(\eta + \lambda_{2})}{\eta} \end{cases}$$

$$(42)$$

• For Mnet, we have

$$\nabla P_{\lambda}(\tilde{u}_{j}) = \begin{cases} \lambda_{1} - \frac{\tilde{u}_{j}}{a} + \lambda_{2}\tilde{u}_{j}, & \text{if } \tilde{u}_{j} \leq a\lambda_{1} \\ \lambda_{2}\tilde{u}_{j}, & \text{if } \tilde{u}_{j} > a\lambda_{1} \end{cases}$$

$$(43)$$

For $\tilde{u}_j \leq a\lambda_1$, the solution of equation (40) is $\frac{a\eta|v_j|-a\lambda_1}{a(\eta+\lambda_2)-1}$. For $\tilde{u}_j > a\lambda_1$, the solution of equation (40) is $\frac{\eta v_j}{\eta+\lambda_2}$. Together with $\tilde{u}_j > 0$ and $\hat{u}_j = \text{sign}(v_j)$, then we have

$$\hat{u}_{j} = \begin{cases} \operatorname{sign}(\boldsymbol{v}_{j}) \cdot \left[\frac{a\eta |\boldsymbol{v}_{j}| - a\lambda_{1}}{a(\eta + \lambda_{2}) - 1} \right]_{+}, & \text{if } |\boldsymbol{v}_{j}| < \frac{a\lambda_{1}(\eta + \lambda_{2})}{\eta} \\ \frac{\eta \boldsymbol{v}_{j}}{\eta + \lambda_{2}}, & \text{if } |\boldsymbol{v}_{j}| \geq \frac{a\lambda_{1}(\eta + \lambda_{2})}{\eta} \end{cases}$$

$$(44)$$

• For Cnet, we have

$$\nabla P_{\lambda}(\tilde{u}_{j}) = \begin{cases} \lambda_{1} + \lambda_{2}\tilde{u}_{j}, & \text{if } \tilde{u}_{j} \leq a\\ \lambda_{2}\tilde{u}_{j}, & \text{if } \tilde{u}_{j} > a \end{cases}$$

$$\tag{45}$$

For $\tilde{u}_j \leq a$, the solution of equation (40) is $\frac{\eta |v_j| - \lambda_1}{\eta + \lambda_2}$. For $\tilde{u}_j > a\lambda_1$, the solution of equation (40) is $\frac{\eta v_j}{\eta + \lambda_2}$.

Together with $\tilde{u}_j > 0$ and $\hat{u}_j = \text{sign}(v_j)$, then we have

$$\hat{u}_{j} = \begin{cases} \operatorname{sign}(\boldsymbol{v}_{j}) \cdot \left[\frac{\eta |\boldsymbol{v}_{j}| - \lambda_{1}}{\eta + \lambda_{2}}\right]_{+}, & \text{if } |\boldsymbol{v}_{j}| < \frac{a(\eta + \lambda_{2})}{\eta} \\ \frac{\eta \boldsymbol{v}_{j}}{\eta + \lambda_{2}}, & \text{if } |\boldsymbol{v}_{j}| \geq \frac{a(\eta + \lambda_{2})}{\eta} \end{cases}$$

$$(46)$$

B Proof of Theorem 2

The proof of Theorem 2 mainly follows the proof framework in Guo et al. (2017). In terms of constrained optimization, we have

$$\min_{\boldsymbol{\beta}, \mathbf{r}} \quad \sum_{i=1}^{n} \mathcal{L}_{\tau, *}(r_i) + P_{\lambda}(|\boldsymbol{\beta}|),$$
s.t. $\mathbf{X}\boldsymbol{\beta} + \mathbf{r} = \mathbf{y}$. (47)

In Guo et al. (2017), they assumed that $\mathcal{L}_{\tau,*}$ is a continuous differentiable function with $\nabla \mathcal{L}_{\tau,*}$ is Lipschitz continuous. We use the following lemma to ensure that the loss function in this paper has such properties.

Lemma 1 (Proposition 2 in Mkhadri et al. (2017)) The smooth quantile $\mathcal{L}_{\tau,c}$ and $\mathcal{L}_{\tau,\kappa}$ are differentiable and have Lipschitz continuous first derivatives, that is,

$$\|\nabla \mathcal{L}_{\tau,c}(u_1) - \nabla \mathcal{L}_{\tau,c}(u_2)\|_2 \le \frac{\max\{\tau, 1 - \tau\}}{c} \|u_1 - u_2\|_2,$$

$$\|\nabla \mathcal{L}_{\tau,\kappa}(u_1) - \nabla \mathcal{L}_{\tau,\kappa}(u_2)\|_2 \le \frac{1}{\kappa} \|u_1 - u_2\|_2,$$

where u_1 and u_2 are two arbitrary real numbers.

Problem (47) has the following augmented Lagrangian,

$$L_{\mu}(\boldsymbol{\beta}, \boldsymbol{r}, \boldsymbol{d}) = \mathcal{L}_{\tau,*}(\boldsymbol{r}) + P_{\lambda}(|\boldsymbol{\beta}|) - \boldsymbol{d}^{\top}(\boldsymbol{X}\boldsymbol{\beta} + \boldsymbol{r} - \boldsymbol{y}) + \frac{\mu}{2} \|\boldsymbol{X}\boldsymbol{\beta} + \boldsymbol{r} - \boldsymbol{y}\|_{2}^{2},$$
(48)

and the iterative steps of LADMM are as follows,

$$\begin{cases}
\boldsymbol{\beta}^{k+1} = \underset{\boldsymbol{\beta}}{\operatorname{arg\,min}} \left\{ P_{\lambda}(|\boldsymbol{\beta}|) + \frac{\mu}{2} \left\| \boldsymbol{X}\boldsymbol{\beta} + \boldsymbol{r}^{k} - \boldsymbol{y} - \boldsymbol{d}^{k}/\mu \right\|_{2}^{2} + \frac{1}{2} \left\| \boldsymbol{\beta} - \boldsymbol{\beta}^{k} \right\|_{S}^{2} \right\}, \\
\boldsymbol{r}^{k+1} = \underset{\boldsymbol{r}}{\operatorname{arg\,min}} \left\{ \mathcal{L}_{\tau,*}(\boldsymbol{r}) + \frac{\mu}{2} \left\| \boldsymbol{X}\boldsymbol{\beta}^{k+1} + \boldsymbol{r} - \boldsymbol{y} - \boldsymbol{d}^{k}/\mu \right\|_{2}^{2} \right\}, \\
\boldsymbol{d}^{k+1} = \boldsymbol{d}^{k} - \mu(\boldsymbol{X}\boldsymbol{\beta}^{k+1} + \boldsymbol{r}^{k+1} - \boldsymbol{y}),
\end{cases} (49)$$

We first demonstrate that the augmented Lagrangian function $L_{\mu}(\boldsymbol{\beta}^{k}, \boldsymbol{r}^{k}, \boldsymbol{d}^{k})$ decreases as the number of iterations increases.

Lemma 2 Let the sequence $w^k = \{\beta^k, r^k, d^k\}$ be generated by the LADMM, then we have

$$L_{\mu}(\boldsymbol{w}^{k+1}) \le L_{\mu}(\boldsymbol{w}^{k}) + \left(\frac{1}{\mu n \min\{c^{2}, \kappa^{2}\}} - \frac{\mu}{2}\right) \|\boldsymbol{r}^{k} - \boldsymbol{r}^{k+1}\|_{2}^{2}.$$
 (50)

Together with $\mu > \sqrt{\frac{2}{n}} \frac{1}{\min\{c,\kappa\}}$, we obtain $\{L_{\mu}(\boldsymbol{w}^k)\}$ is monotonically nonincreasing.

Proof The optimality conditions for the k + 1-iteration of LADMM is

$$\begin{cases}
\mathbf{0} \in \partial P_{\lambda}(|\boldsymbol{\beta}^{k+1}|) - \boldsymbol{X}^{\top} \boldsymbol{d}^{k} + \mu \boldsymbol{X}^{\top} (\boldsymbol{X} \boldsymbol{\beta}^{k+1} + \boldsymbol{r}^{k} - \boldsymbol{y}) + \boldsymbol{S} (\boldsymbol{\beta}^{k+1} - \boldsymbol{\beta}^{k}), \\
\mathbf{0} = \nabla \mathcal{L}_{\tau,*}(\boldsymbol{r}^{k+1}) - \boldsymbol{d}^{k} + \mu (\boldsymbol{X} \boldsymbol{\beta}^{k+1} + \boldsymbol{r}^{k+1} - \boldsymbol{y}), \\
\boldsymbol{d}^{k+1} = \boldsymbol{d}^{k} - \mu (\boldsymbol{X} \boldsymbol{\beta}^{k+1} + \boldsymbol{r}^{k+1} - \boldsymbol{y}).
\end{cases} (51)$$

Using the last equality and rearranging terms, we obtain

$$\begin{cases}
\mathbf{0} \in \partial P_{\lambda}(|\boldsymbol{\beta}^{k+1}|) - \boldsymbol{X}^{\top} \boldsymbol{d}^{k+1} + \mu \boldsymbol{X}^{\top} (\boldsymbol{r}^{k} - \boldsymbol{r}^{k+1}) + \boldsymbol{S}(\boldsymbol{\beta}^{k+1} - \boldsymbol{\beta}^{k}), \\
\nabla \mathcal{L}_{\tau,*}(\boldsymbol{r}^{k+1}) = \boldsymbol{d}^{k+1}.
\end{cases} (52)$$

From the definition of the augmented Lagrangian function L_{μ} , it follows that

$$L_{\mu}(\boldsymbol{\beta}^{k+1}, \boldsymbol{r}^{k+1}, \boldsymbol{d}^{k+1}) = L_{\mu}(\boldsymbol{\beta}^{k+1}, \boldsymbol{r}^{k+1}, \boldsymbol{d}^{k}) + \langle \boldsymbol{d}^{k} - \boldsymbol{d}^{k+1}, \boldsymbol{X} \boldsymbol{\beta}^{k+1} + \boldsymbol{r}^{k+1} - \boldsymbol{y} \rangle$$

$$= L_{\mu}(\boldsymbol{\beta}^{k+1}, \boldsymbol{r}^{k+1}, \boldsymbol{d}^{k}) + \frac{1}{\mu} \|\boldsymbol{d}^{k} - \boldsymbol{d}^{k+1}\|_{2}^{2},$$
(53)

and

$$L_{\mu}(\boldsymbol{\beta}^{k+1}, \boldsymbol{r}^{k}, \boldsymbol{d}^{k}) - L_{\mu}(\boldsymbol{\beta}^{k+1}, \boldsymbol{r}^{k+1}, \boldsymbol{d}^{k}) = (\mathcal{L}_{\tau,*}(\boldsymbol{r}^{k}) - \mathcal{L}_{\tau,*}(\boldsymbol{r}^{k+1})) - \langle \boldsymbol{d}^{k}, \boldsymbol{r}^{k} - \boldsymbol{r}^{k+1} \rangle + \frac{\mu}{2} \left[\|\boldsymbol{X}\boldsymbol{\beta}^{k+1} + \boldsymbol{r}^{k} - \boldsymbol{y}\|_{2}^{2} - \|\boldsymbol{X}\boldsymbol{\beta}^{k+1} + \boldsymbol{r}^{k+1} - \boldsymbol{y}\|_{2}^{2} \right].$$
 (54)

Since $\mathcal{L}_{\tau,*}$ is a convex function and $\mathbf{d}^{k+1} = \mathbf{d}^k - \mu(\mathbf{X}\boldsymbol{\beta}^{k+1} + \mathbf{r}^{k+1} - \mathbf{y})$, we have

$$\begin{cases}
\mathcal{L}_{\tau,*}(\boldsymbol{r}^{k}) - \mathcal{L}_{\tau,*}(\boldsymbol{r}^{k+1}) \geq \langle \nabla \mathcal{L}_{\tau,*}(\boldsymbol{r}^{k+1}), \boldsymbol{r}^{k} - \boldsymbol{r}^{k+1} \rangle, \\
\boldsymbol{X}\boldsymbol{\beta}^{k+1} + \boldsymbol{r}^{k} - \boldsymbol{y} = (\boldsymbol{d}^{k} - \boldsymbol{d}^{k+1})/\mu + (\boldsymbol{r}^{k} - \boldsymbol{r}^{k+1}), \\
\boldsymbol{X}\boldsymbol{\beta}^{k+1} + \boldsymbol{r}^{k+1} - \boldsymbol{y} = (\boldsymbol{d}^{k} - \boldsymbol{d}^{k+1})/\mu.
\end{cases} (55)$$

Note that $\nabla \mathcal{L}_{\tau,*}(\mathbf{r}^{k+1}) = \mathbf{d}^{k+1}$ and insert Equation (55) into Equation (54) yields

$$L_{\mu}(\boldsymbol{\beta}^{k+1}, \boldsymbol{r}^{k+1}, \boldsymbol{d}^{k}) \le L_{\mu}(\boldsymbol{\beta}^{k+1}, \boldsymbol{r}^{k}, \boldsymbol{d}^{k}) - \frac{\mu}{2} \|\boldsymbol{r}^{k} - \boldsymbol{r}^{k+1}\|_{2}^{2}.$$
 (56)

Combining Equations (56) and (53), we obtain

$$L_{\mu}(\boldsymbol{\beta}^{k+1}, \boldsymbol{r}^{k+1}, \boldsymbol{d}^{k+1}) \leq L_{\mu}(\boldsymbol{\beta}^{k+1}, \boldsymbol{r}^{k}, \boldsymbol{d}^{k}) - \frac{\mu}{2} \|\boldsymbol{r}^{k} - \boldsymbol{r}^{k+1}\|_{2}^{2} + \frac{1}{\mu} \|\boldsymbol{d}^{k} - \boldsymbol{d}^{k+1}\|_{2}^{2}.$$
 (57)

From the Lemma 1 and recall that $\mathcal{L}_{\tau,*}(\mathbf{r}) = \frac{1}{n} \sum_{i=1}^{n} \mathcal{L}_{\tau,*}(\mathbf{r}_i)$, we have

$$\|\boldsymbol{d}^{k} - \boldsymbol{d}^{k+1}\|_{2} = \|\nabla \mathcal{L}_{\tau,*}(\boldsymbol{r}^{k}) - \nabla \mathcal{L}_{\tau,*}(\boldsymbol{r}^{k+1})\|_{2} \le \frac{1}{\sqrt{n}\min\{c,\kappa\}} \|\boldsymbol{r}^{k} - \boldsymbol{r}^{k+1}\|_{2}.$$
 (58)

Consequently, we have

$$L_{\mu}(\boldsymbol{\beta}^{k+1}, \boldsymbol{r}^{k+1}, \boldsymbol{d}^{k+1}) \le L_{\mu}(\boldsymbol{\beta}^{k+1}, \boldsymbol{r}^{k}, \boldsymbol{d}^{k}) + \left(\frac{1}{\mu n \min\{c^{2}, \kappa^{2}\}} - \frac{\mu}{2}\right) \|\boldsymbol{r}^{k} - \boldsymbol{r}^{k+1}\|_{2}^{2}.$$
 (59)

Note that $\boldsymbol{\beta}^{k+1}$ is the value that minimizes $L_{\mu}(\boldsymbol{\beta}, \boldsymbol{r}^{k}, \boldsymbol{d}^{k}) + \frac{1}{2} \|\boldsymbol{\beta} - \boldsymbol{\beta}^{k}\|_{\boldsymbol{S}}^{2}$ and \boldsymbol{S} is a positive-definite matrix, then we get

$$L_{\mu}(\boldsymbol{\beta}^{k+1}, \boldsymbol{r}^{k}, \boldsymbol{d}^{k}) \leq L_{\mu}(\boldsymbol{\beta}^{k}, \boldsymbol{r}^{k}, \boldsymbol{d}^{k}). \tag{60}$$

As a result,

$$L_{\mu}(\boldsymbol{\beta}^{k+1}, \boldsymbol{r}^{k+1}, \boldsymbol{d}^{k+1}) \leq L_{\mu}(\boldsymbol{\beta}^{k}, \boldsymbol{r}^{k}, \boldsymbol{d}^{k}) + \left(\frac{1}{\mu n \min\{c^{2}, \kappa^{2}\}} - \frac{\mu}{2}\right) \|\boldsymbol{r}^{k} - \boldsymbol{r}^{k+1}\|_{2}^{2}.$$
(61)

Since we assume that $\mu > \sqrt{\frac{2}{n}} \frac{1}{\min\{c,\kappa\}}$, then we have $\left(\frac{1}{\mu n \min\{c^2,\kappa^2\}} - \frac{\mu}{2}\right) < 0$, which implies that $\{L_{\mu}(\boldsymbol{w}^k)\}$ is monotonically nonincreasing.

Next, we will prove that the iterative sequences generated by LADMM are bounded.

Lemma 3 With $\mu > \sqrt{\frac{2}{n}} \frac{1}{\min\{c,\kappa\}}$ and $\mathbf{X}^{\top} \mathbf{X} > \underline{\mu} \mathbf{I}_p(\underline{\mu} > 0)$, if $P_{\lambda}(\boldsymbol{\beta})$ is the SCAD,MCP and capped- ℓ_1 , then the sequence $\mathbf{w}^k = \{\boldsymbol{\beta}^k, \mathbf{r}^k, \mathbf{d}^k\}$ is generated by LADMM is bounded.

Proof Since $\{L_{\mu}(\boldsymbol{w}^k)\}$ is monotonically nonincreasing, we have

$$L_{\mu}(\boldsymbol{w}^{0}) \geq L_{\mu}(\boldsymbol{w}^{k}) = \mathcal{L}_{\tau,*}(\boldsymbol{r}^{k}) + P_{\lambda}(|\boldsymbol{\beta}^{k}|) - \langle \boldsymbol{d}^{k}, \boldsymbol{X}\boldsymbol{\beta}^{k} + \boldsymbol{r}^{k} - \boldsymbol{y} \rangle + \frac{\mu}{2} \left\| \boldsymbol{X}\boldsymbol{\beta}^{k} + \boldsymbol{r}^{k} - \boldsymbol{y} \right\|_{2}^{2}$$
$$= \mathcal{L}_{\tau,*}(\boldsymbol{r}^{k}) + P_{\lambda}(|\boldsymbol{\beta}^{k}|) + \frac{\mu}{2} \left\| \boldsymbol{X}\boldsymbol{\beta}^{k} + \boldsymbol{r}^{k} - \boldsymbol{y} - \boldsymbol{d}^{k}/\mu \right\|_{2}^{2} - \frac{\|\boldsymbol{d}^{k}\|_{2}^{2}}{2\mu}$$
(62)

Since $P_{\lambda}(|\boldsymbol{\beta}^{k}|)$ and $\nabla P_{\lambda}(|\boldsymbol{\beta}^{k}|) = \boldsymbol{d}^{k}$ are bounded, then $\mathcal{L}_{\tau,*}(\boldsymbol{r}^{k})$ and $\frac{\mu}{2} \|\boldsymbol{X}\boldsymbol{\beta}^{k} + \boldsymbol{r}^{k} - \boldsymbol{y} - \boldsymbol{d}^{k}/\mu\|_{2}^{2}$ must be bounded. Note that if $\|\boldsymbol{r}^{k}\|_{2} \to \infty$, $\mathcal{L}_{\tau,*}(\boldsymbol{r}^{k}) \to \infty$, then \boldsymbol{r}^{k} is bounded. Note also that $\boldsymbol{X}^{\top}\boldsymbol{X}$, then as long as $\boldsymbol{X}^{\top}\boldsymbol{X} > \underline{\mu}\boldsymbol{I}_{p}$, $\boldsymbol{\beta}^{k}$ must be bounded. Consequently, \boldsymbol{w}^{k} is bounded.

Remark 2 This conclusion holds true for penalties such as Mnet, Snet and Cnet, even without the condition $X_m^{\top} X_m > \mu I_p$.

Now, we will derive convergence conclusions $\lim_{k\to+\infty} \|\boldsymbol{w}^k - \boldsymbol{w}^{k+1}\|_2 = 0$, which is similar to Guan et al. (2018).

Lemma 4 Let the sequence $w^k = \{\beta^k, r^k, d^k\}$ be generated by LADMM, then

$$\sum_{k=0}^{\infty} \| \boldsymbol{w}^k - \boldsymbol{w}^{k+1} \|_2^2 \le +\infty, \tag{63}$$

and as a consequence, $\lim_{k\to+\infty} \|\boldsymbol{w}^k - \boldsymbol{w}^{k+1}\|_2 = 0$

Proof Since $\{\boldsymbol{w}^k\}$ is bounded, it has at least one cluster point. Let \boldsymbol{w}^* be a cluster point of $\{\boldsymbol{w}^k\}$ and let $\{\boldsymbol{w}^{k_j}\}$ be the subsequence converging to it, i.e. $\boldsymbol{w}^{k_j} \to \boldsymbol{w}^*$. Since L_{μ} is the continuous function, and hence

$$L_{\mu}(\boldsymbol{w}^{k_j}) \geq L_{\mu}(\lim_{j \to \infty} \boldsymbol{w}^{k_j}) = L_{\mu}(\boldsymbol{w}^*)$$

As a result, $L_{\mu}(\mathbf{w}^{k_j})$ has a lower bound, which, together with the fact that $L_{\mu}(\mathbf{w}^{k_j})$ is nonincreasing, means that $L_{\mu}(\mathbf{w}^{k_j})$ is convergent. Further, we can conclude that $L_{\mu}(\mathbf{w}^k)$ converges and $L_{\mu}(\mathbf{w}^k) \geq L_{\mu}(\mathbf{w}^k)$.

Rearranging terms of Equation (50) yields

$$\left(\frac{\mu}{2} - \frac{1}{\mu n \min\{c^2, \kappa^2\}}\right) \|\boldsymbol{r}^k - \boldsymbol{r}^{k+1}\|_2^2 \le L_{\mu}(\boldsymbol{w}^k) - L_{\mu}(\boldsymbol{w}^{k+1}),$$

and summing up for $k = 0, ..., +\infty$, it follows

$$\left(\frac{\mu}{2} - \frac{1}{\mu n \min\{c^2, \kappa^2\}}\right) \sum_{k=0}^{+\infty} \|\boldsymbol{r}^k - \boldsymbol{r}^{k+1}\|_2^2 \le L_{\mu}(\boldsymbol{w}^0) - L_{\mu}(\boldsymbol{w}^*) < +\infty.$$

Since $\left(\frac{\mu}{2} - \frac{1}{\mu n \min\{c^2, \kappa^2\}}\right) > 0$, we obtain $\sum_{k=0}^{+\infty} \|\boldsymbol{r}^k - \boldsymbol{r}^{k+1}\|_2^2 < +\infty$. Consequently, it follows from Equation (58) that $\sum_{k=0}^{+\infty} \|\boldsymbol{d}^k - \boldsymbol{d}^{k+1}\|_2^2 < +\infty$. Hence, to complete the proof, we just need to prove that $\sum_{k=0}^{+\infty} \|\boldsymbol{\beta}^k - \boldsymbol{\beta}^{k+1}\|_2^2 < +\infty$. For the m-th local machine, we have

$$\left\{egin{aligned} oldsymbol{d}_m^{k+1} &= oldsymbol{d}_m^k - \mu(oldsymbol{X}_moldsymbol{eta}^{k+1} + oldsymbol{r}_m^{k+1} - oldsymbol{y}_m), \ oldsymbol{d}_m^k &= oldsymbol{d}_m^{k-1} - \mu(oldsymbol{X}_moldsymbol{eta}^k + oldsymbol{r}_m^k - oldsymbol{y}_m), \end{aligned}
ight.$$

and hence

$$d_m^{k+1} - d_m^k = d_m^k - d_m^{k-1} - \mu X_m (\beta^{k+1} - \beta^k) - \mu (r_m^{k+1} - r_m^k).$$

It then follows that

$$\|\mu \mathbf{X}_{m}(\boldsymbol{\beta}^{k+1} - \boldsymbol{\beta}^{k})\|_{2}^{2} = \|(\mathbf{d}_{m}^{k} - \mathbf{d}_{m}^{k-1}) - (\mathbf{d}_{m}^{k+1} - \mathbf{d}_{m}^{k}) - \mu(\mathbf{r}_{m}^{k+1} - \mathbf{r}_{m}^{k})\|_{2}^{2}$$

$$\leq 3(\|\mathbf{d}_{m}^{k} - \mathbf{d}_{m}^{k-1}\|_{2}^{2} + \|\mathbf{d}_{m}^{k+1} - \mathbf{d}_{m}^{k}\|_{2}^{2} + \|\mu(\mathbf{r}_{m}^{k+1} - \mathbf{r}_{m}^{k})\|_{2}^{2})$$
(64)

Since we assume $X_m^{\top} X_m > \underline{\mu} I_p$, we have

$$\|\mu \mathbf{X}_{m}(\boldsymbol{\beta}^{k+1} - \boldsymbol{\beta}^{k})\|_{2}^{2} \ge \mu^{2} \mu \|\boldsymbol{\beta}^{k+1} - \boldsymbol{\beta}^{k}\|_{2}^{2}.$$
 (65)

Then, combining Equations (64) and (65), we can obtain

$$\sum_{k=0}^{+\infty} \|\beta^k - \beta^{k+1}\|_2^2 < +\infty.$$

Therefore, we have proved $\sum_{k=1}^{\infty} \| \boldsymbol{w}^k - \boldsymbol{w}^{k+1} \|_2^2 \leq \infty$.

However, this conclusion $\lim_{k\to+\infty} \|\boldsymbol{w}^k - \boldsymbol{w}^{k+1}\|_2 = 0$ only ensures that the difference between \boldsymbol{w}^k and \boldsymbol{w}^{k+1} is close to 0, but it does not guarantee that \boldsymbol{w}^k converges. From Lemma 3, we know that \boldsymbol{w}^k has at least one limit point. Next, we will prove some properties about the limit points.

Lemma 5 Let $S(\mathbf{w}^{\infty})$ denote the set of the limit points of $\{\mathbf{w}^k\}$ and $C(\mathbf{w}^*)$ denote the set of critical points of $L_{\mu}(\mathbf{w})$. Then, we have $S(\mathbf{w}^{\infty}) \subset C(\mathbf{w}^*)$, and $L_{\mu}(\mathbf{w})$ is finite and constant on $S(\mathbf{w}^{\infty})$.

Proof We say \mathbf{w}^* is the critical point of $L_{\mu}(\mathbf{w})$, if it satisfies

$$\begin{cases}
\mathbf{X}^{\top} \mathbf{d}^* \in \partial P_{\lambda}(|\boldsymbol{\beta}^*|), \\
\mathbf{d}^* = \nabla \mathcal{L}_{\tau,*}(\mathbf{r}^*), \\
\mathbf{0} = \mathbf{X}\boldsymbol{\beta}^* + \mathbf{r}^* - \mathbf{y}.
\end{cases} (66)$$

Recall the optimality conditions for the k+1-iteration of LADMM in (51), we get

$$\begin{cases}
\mathbf{0} \in \partial P_{\lambda}(|\boldsymbol{\beta}^{k+1}|) - \boldsymbol{X}^{\top} \boldsymbol{d}^{k+1} + \boldsymbol{S}(\boldsymbol{\beta}^{k+1} - \boldsymbol{\beta}^{k}), \\
\mathbf{0} = \nabla \mathcal{L}_{\tau,*}(\boldsymbol{r}^{k+1}) - \boldsymbol{d}^{k+1}, \\
\boldsymbol{d}^{k+1} = \boldsymbol{d}^{k} - \mu(\boldsymbol{X}\boldsymbol{\beta}^{k+1} + \boldsymbol{r}^{k+1} - \boldsymbol{y}).
\end{cases} (67)$$

For any limit point \mathbf{w}^{∞} , from Lemma 4 and (67), we have

$$\begin{cases}
\mathbf{X}^{\top} \mathbf{d}^{\infty} \in \partial P_{\lambda}(|\boldsymbol{\beta}^{\infty}|), \\
\mathbf{d}^{\infty} = \nabla \mathcal{L}_{\tau,*}(\mathbf{r}^{\infty}), \\
\mathbf{0} = \mathbf{X} \boldsymbol{\beta}^{\infty} + \mathbf{r}^{\infty} - \mathbf{y}.
\end{cases} (68)$$

As a consequence, $S(\boldsymbol{w}^{\infty}) \subset S(\boldsymbol{w}^*)$. Note that $L_{\mu}(\boldsymbol{w}^k)$ is nonincreasing and convergent, thus we have $L_{\mu}(\boldsymbol{w})$ is finite and constant on $S(\boldsymbol{w}^{\infty})$.

Now, we are ready to prove Theorem 2. Despite the LADMM algorithm having an additional term of $\frac{1}{2} \| \boldsymbol{\beta} - \boldsymbol{\beta}^k \|_S^2$ compared to the ADMM algorithm in Guo et al. (2017), the convergence proof is identical to that of Theorem 3.1 in Guo et al. (2017). Following the same steps as the proof, we also can conclude that

$$\sum_{k=0}^{+\infty} \| \boldsymbol{w}^{k+1} - \boldsymbol{w}^k \|_2 < +\infty, \tag{69}$$

then $\{\boldsymbol{w}^k\}$ is a Cauchy sequence and converges. Together with Lemma 5, $\{\boldsymbol{w}^k\}$ converges to a critical point of $L_{\mu}(\boldsymbol{w})$.

C Supplementary Numerical Experiments

C.1 Supplementary Experiments for Section 4.1

In this subsection, we compare the performance of LADMM and other ADMMs under MCP penalty term. Table 6 demonstrates the results for the nonparallel version (M = 1), while Table 7 shows the results for the parallel version (M > 1).

Table 6: Comparison of various ADMMs with MCP penalty of different data sizes.

(n,p)	(300	00,100	00)			(100	0,3000	00)		
$\tau = 0.3$	P1	P2	AE	Ite	Time	P1	P2	AE	Ite	Time
QPADM	100	100	0.013(0.01)	95.9(9.8)	34.67(5.7)	0	100	6.68(0.97)	500(0.0)	2013.4(59.4)
QPADMslack	100	100	0.042(0.02)	47.2(6.1)	38.72(5.3)	0	100	7.13(0.89)	226(13.8)	1234.8(36.7)
FSLADMM	100	100	0.015(0.03)	500(0.0)	161.32(10.9)	100	100	0.69(0.07)	500(0.0)	129.5(11.3)
LADMM	100	100	0.014(0.01)	39.5 (3.0)	31.87(3.9)	100	100	0.38(0.05)	123(10.2)	56.3(4.6)
$\tau = 0.5$	P1	P2	AE	Ite	Time	P1	P2	AE	Ite	Time
QPADM	0	100	0.011(0.01)	87.9(8.5)	29.58(5.1)	0	100	5.92(0.82)	500(0.0)	1967.5(60.1)
QPADMslack	0	100	0.038(0.03)	41.7(5.5)	32.39(4.8)	0	100	7.24(0.78)	232(12.7)	1094.7(40.2)
FSLADMM	0	100	0.015(0.04)	500(0.0)	148.95(9.7)	0	100	0.64(0.06)	500(0.0)	131.8(12.5)
LADMM	0	100	0.012(0.01)	$35.2\ (2.7)$	28.59(3.5)	0	100	0.35(0.03)	119(9.1)	57.4(5.1)
$\tau = 0.7$	P1	P2	AE	Ite	Time	P1	P2	AE	Ite	Time
QPADM	100	100	0.016(0.02)	99.2(9.3)	38.54(6.1)	100	100	6.81(0.77)	500(0.0)	2123.7(58.9)
QPADMslack	100	100	0.049(0.05)	48.5(5.7)	42.21(5.6)	100	100	6.93(0.72)	262(15.7)	1182.6(49.3)
FSLADMM	100	100	0.021(0.04)	500(0.0)	157.17(9.9)	100	100	0.72(0.06)	500(0.0)	136.5(13.0)
LADMM	100	100	0.018(0.01)	40.8(3.1)	30.27(3.2)	100	100	0.39(0.03)	130(9.9)	60.2(4.9)

^{*} The meanings of the notations used in this table are as follows: P1 (%): proportion that x_1 is selected; P2 (%): proportion that x_6 , x_{12} , x_{15} , and x_{20} are selected; AE: absolute estimation error; Ite: number of iterations; Time (s): running time. Numbers in the parentheses represent the corresponding standard deviations. The optimal solution is represented in bold.

Table 7: Comparison of various parallel ADMMs with MCP penalty.

(n = 500000, p = 1000)	$\tau = 0.4$				$\tau = 0.5$			
M=5	Nonzero	AE	Ite	Time	Nonzero	AE	Ite	Time
QPADM QPADMslack LADMM	30.8(2.8) 28.1(3.1) 5.3(0.3)	0.048(0.005) 0.045(0.006) 0.029(0.001)	492.9(39.6) 335.1(26.8) 79.5 (4.2)	204.7(25.7) 127.2(16.5) 41.2(4.1)	25.7(2.2) 24.1(1.8) 4.1(0.07)	0.043(0.004) 0.042(0.005) 0.024(0.001)	495.9(39.7) 347.2(45.1) 82.6 (5.3)	212.6(30.2) 135.2(15.9) 39.7(3.8)
M = 20	Nonzero	AE	Ite	Time	Nonzero	AE	Ite	Time
QPADM QPADMslack LADMM	32.6(3.5) 29.4(3.4) 5.3(0.3)	0.051(0.06) 0.048(0.07) 0.029(0.001)	500(0.0) 341.4(35.2) 79.5 (4.2)	129.8(12.6) 62.9(8.5) 28.5(3.2)	28.3(2.4) 25.9(2.1) 4.1(0.07)	0.048(0.05) 0.047(0.05) 0.024(0.001)	500(0.0) 402.3(51.5) 82.6 (5.3)	129.6(15.0) 72.9(7.8) 27.5(3.5)
M = 100	Nonzero	AE	Ite	Time	Nonzero	AE	Ite	Time
QPADM QPADMslack LADMM	35.1(4.0) 32.7(3.8) 5.3(0.3)	0.076(0.08) 0.069(0.06) 0.029(0.001)	500(0.0) 448.5(56.2) 79.5 (4.2)	48.54(4.1) 18.21(2.5) 19.27(2.6)	30.8(2.7) 28.6(3.2) 4.1(0.07)	0.052(0.06) 0.049(0.06) 0.024(0.001)	500(0.0) 441.4(62.1) 82.6 (5.3)	38.4(3.9) 20.1(2.5) 20.7(2.2)

^{*} P1 and P2 are not presented in Table 2 because all methods have a value of 100 for these two metrics. Theorem 1 ensures that the Nonzero, AE, and Ite of LADMM are not affected by the M value.

C.2 Supplementary Experiments for Section 4.2

In this subsection, we compare the performance of LADMM and ILAMM under MCP and Capped- ℓ_1 penalty terms. Table 8 demonstrates the results.

Table 8: Comparison of LS-MCP and Huber-MCP Calculated by LADMM and ILAMM

		MC	Р			Cap	$\operatorname{ped-}\ell$	1	
Algorithm	(n,p)	FP	FN	AE	Time	FP	FN	AE	Time
ILAMM	(100,1000) (100,10000) (1000,10000) (10000,10000)	0 0 0 0	1 2 2 0	0.43(0.08) 0.61(0.10) 0.53(0.08) 0.09(0.02)	8.6(0.9) 164.2(10.6) 252.5(21.9) 1846.8(138.6)	0 0 0 0	1 2 2 0	0.52(0.07) 0.67(0.12) 0.58(0.09) 0.13(0.04)	9.1(1.0) 157.3(9.8) 283.8(27.5) 2014.5(142.4)
Algorithm	(n,p)	FP	FN	AE	Time	FP	FN	AE	Time
LADMM	(100,1000) (100,10000) (1000,10000) (10000,10000)	0 0 0 0	0 0 0 0	0.44(0.04) 0.52(0.05) 0.48(0.07) 0.05(0.01)	1.4(0.07) 7.6(1.12) 15.8(2.65) 35.7(5.48)	0 0 0 0	0 0 0 0	$0.39(0.02) \\ 0.45(0.04) \\ 0.41(0.05) \\ 0.04(0.01)$	1.2(0.09) 5.5(1.01) 13.1(1.98) 25.5(4.70)

^{*} False Positive (FP) refers to the number of variables with a coefficient of zero that are mistakenly included in the final model, while False Negative (FN) refers to the number of variables with non-zero coefficients that are omitted from the model.

C.3 Supplementary Experiments for Section 4.3

In this subsection, we compare the performance of LADMM and cdaSQR under Mnet penalty term. Table 9 demonstrates the results. For Cnet penalty term, cdaSQR can not solve it. We only visualize the results of LADMM solving Cnet in Figure 6.

Table 9: Comparison of LADMM and cdaSQR with $\delta = 0.5$ and $\tau = 0.5$

		cdaSe	QR			LAI	OMM		
Loss	(n, p)	FP	FN	AE	Time	FP	FN	AE	Time
$\mathcal{L}_{ au,c}$	(5000,500) (10000,1000) (20000,2000)	1.96 2.10 3.08	6.48 7.21 9.59	0.36(0.03) 0.48(0.05) 0.62(0.07)	3.46(0.23) 5.13(0.61) 24.36(3.28)	0 0 0	0.08 0.09 0.10	0.37(0.02) 0.45(0.04) 0.53(0.06)	3.72(0.29) 4.85(0.55) 19.82(2.7)
Loss	(n,p)	FP	FN	AE	Time	FP	FN	AE	Time
$\mathcal{L}_{ au,\kappa}$	(5000,500) (10000,1000) (20000,2000)	2.01 2.54 2.92	6.07 7.42 9.43	0.39(0.02) 0.51(0.06) 0.64(0.08)	4.12(0.32) 6.27(0.95) 26.72(3.73)	0 0 0	$0.05 \\ 0.06 \\ 0.08$	0.42(0.03) 0.46(0.05) 0.57(0.06)	3.64(0.32) $4.58(0.57)$ $21.36(2.9)$

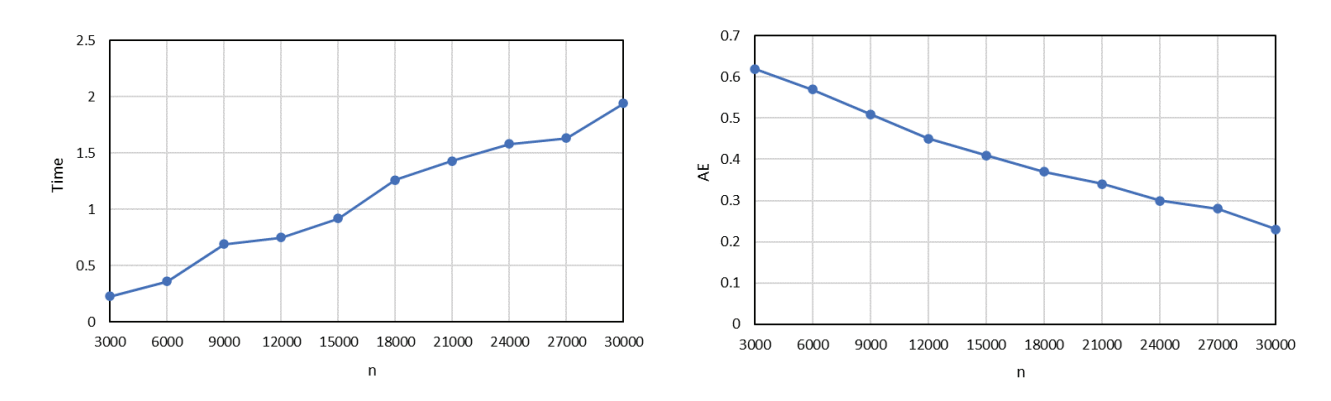


Figure 6: Variation of computing time and AE with n

C.4 Supplementary Experiments for Section 5

In this subsection, we compare the performance of several parallel ADMM algorithms in an online publicly available dataset. The results are presented in Table 10.

Table 10: Analysis of the news popularity data under the MCP penalty.

	Algorithm	x_{14}	x_{27}	Nonzero	FP	Ite	Time
	QRADM	-0.023(0.003)	0.056(0.004)	33.9(2.30)	0.20(0.01)	230.2(44.3)	0.36(0.08)
$\tau = 0.5$	QRADMslack	-0.020(0.001)	0.052(0.002)	35.1(1.95)	0.20(0.01)	118.3(10.6)	0.21(0.06)
	$LADMM_{\rho}$	-0.011(0.001)	0.024(0.001)	12.3(0.66)	0.18(0.01)	73.6(5.9)	0.10(0.01)
	$LADMM_{\mathcal{L}_{\tau,c},\delta=1}$	-0.013(0.001)	0.026(0.002)	13.1(0.56)	0.19(0.01)	71.5(6.1)	0.13(0.01)
	$LADMM_{\mathcal{L}_{\tau,\kappa},\delta=1}$	-0.011(0.001)	0.023(0.001)	13.8(0.72)	0.19(0.01)	80.2(6.3)	0.12(0.01)
	Algorithm	x_{14}	x_{27}	Nonzero	FP	Ite	Time
	Algorithm QRADM	x_{14} -0.138(0.013)	x_{27} $0.317(0.009)$	Nonzero 38.9(2.92)	FP 0.24(0.01)	Ite 500(0.00)	Time 0.93(0.12)
$\tau = 0.9$							
$\tau = 0.9$	QRADM	-0.138(0.013)	0.317(0.009)	38.9(2.92)	0.24(0.01)	500(0.00)	0.93(0.12)
$\tau = 0.9$	QRADM QRADMslack	-0.138(0.013) -0.120(0.009)	0.317(0.009) 0.289(0.007)	38.9(2.92) 40.1(1.85)	0.24(0.01) 0.24(0.01)	500(0.00) 472.3(51.6)	0.93(0.12) 0.56(0.08)